Fermi National Accelerator Laboratory

FERMILAB-Pub-87/227-A
December 1987

COSMIC STRINGS AND THE MICROWAVE SKY I: ANISOTROPY FROM MOVING STRINGS[1]

ALBERT STEBBINS

NASA/Fermilab Astrophysics Center
Fermi National Accelerator Laboratory

ABSTRACT. In this paper we develop a method for calculating the component of the microwave anisotropy around cosmic string loops due to their rapidly changing gravitational fields. The method is only valid for impact parameters from the string much smaller than the horizon size at the time the photon passes the string. The methods developed allows one to calculate the temperature pattern around *arbitrary* string configurations numerically in terms of one dimensional integrals. This method is applied to temperature jump across a string, confirming and extending previous work. It is also applied to cusps and kinks on strings, and to determining the temperature pattern far from a string loop. The temperature pattern around a few loop configurations is explicitly calculated. The fractional temperature deviation near the string is typically 5-10 $G\mu/c^2$. Very large anisotropies are produced near cusps and kinks. These large anisotropies only occur over a relatively small angular area on the sky. Comparison with the work of Brandenberger, Albrecht, and Turok indicates that these have overestimated the MBR anisotropy from gravitational radiation emitted from loops.

I. INTRODUCTION

Recently much attention has been paid to the possibility that linelike topological defects called cosmic strings could be the cause of inhomogeneities in the universe (see Vilenkin 1985 for a review). These topological defects are produced naturally in some, but not all, gauge theories as one goes from very high temperatures to very low temperatures. Given a very homogeneous universe at some very early time and the subsequent production of strings in a phase transition one would naturally produce nonlinear inhomogeneities in any component whose effective sound speed fell below some critical value. This, in our universe, could produce inhomogeneities in the baryonic component and in any sufficiently cold nonbaryonic component. If the strings only interact gravitationally with the matter then the statistical properties of the structure produced will depend only on their fixed mass per unit length, μ. Additional uncertainties come from our ignorance about the contents of the universe (i.e. possible non-baryonic matter) as well as the curvature of the universe (i.e. Ω_0). To this we must add our ignorance about the behavior of string networks, nonlinear gravitational clustering, baryonic dissipation, primordial star formation, etc. Thus, as with any theory of the formation of structure, there are large uncertainties in determining whether observations of the large scale structure match any theory. Gross inconsistencies are required to convincingly rule a theory out. One thing we may say about strings is that if the mass per unit length of the string is too small then it could not possibly induce gravitational condensations with velocity dispersions as large as those seen in clusters of galaxies (Turok and Brandenberger 1986, Stebbins 1986). Typical estimates are

$$\tilde{\mu} \gtrsim 10^{-6} \qquad \text{where} \qquad \tilde{\mu} \equiv \frac{G\mu}{c^2}. \tag{1.1}$$

[1]to appear *THE ASTROPHYSICAL JOURNAL* 15 April 1988

Operated by Universities Research Association Inc. under contract with the United States Department of Energy

(Here $\tilde{\mu}$ is equivalent to $G\mu$ used in most other works in which they take $c = 1$.) In the standard string model, in which strings only interact gravitationally, they produce copious amount of long wavelength gravitational waves which would disrupt the observed timing of the millisecond pulsar if μ is too large (Hogan and Rees 1984). In addition, estimates of the microwave background radiation (MBR) anisotropy produced by strings place additional upper limits on μ (Kaiser and Stebbins 1984; Brandenberger and Turok 1986; Traschen, Turok, and Brandenberger 1986, Brandenberger, Albrecht, and Turok 1986). Typical estimates from both the MBR anisotropy and the pulsar timing are

$$\tilde{\mu} \lesssim 10^{-5}. \tag{1.2}$$

Since the anisotropies typically scale linearly with $\tilde{\mu}$, we see that the predicted anisotropies are within an order of magnitude of present detection sensitivities.

If one were able to detect and measure the statistical properties of the MBR anisotropies this would provide another probe of primordial density inhomogeneities. In fact, in most theories of the formation of structure, the predictions of the statistical properties of the MBR anisotropy is much more straightforward than the predictions of the distribution of galaxies. The MBR anisotropy is, in this sense, a better probe of the primordial inhomogeneities than the large-scale structure. Of course, we will have to wait for improvements in detector sensitivities before primordial fluctuations can be studied in this way. In theories in which the initial fluctuations are Gaussian the properties of the predicted anisotropies may be calculated in a straightforward way and have been well studied. This is not the case for strings. The anisotropy produced by specific geometries have been studied (Kaiser and Stebbins 1984, Vachaspati 1987, Chase 1986). Some estimates of the statistical properties of some component of the anisotropies have also been studied. However, in these studies, the normalization was estimated only crudely. Furthermore, the dominant component of the anisotropy is likely to be that produced by the rapidly changing gravitational fields of strings (Brandenberger, Albrecht, and Turok 1986), and the statistical properties of this is not well understood. Because of the non-Gaussian nature of the anisotropies, the necessary sum over realizations probably cannot be performed analytically. The approach to calculating anisotropies suggested here is to develop techniques for calculating anisotropies for arbitrary geometries and then to apply this technique with statistical realizations of string configurations generated numerically, and thus to obtain the expected distribution of anisotropies.

The purpose of this paper is to develop the machinery for calculating the anisotropy produced around an arbitrary loop in Minkowski space illuminated by a constant brightness background. This should produce a good approximation to the anisotropy produced by loops much smaller than the horizon. This correspondence is true whether or not the loop we see projected on our sky is from small or large redshift; it is only required that we see the loop in front of the surface of last scattering which is probably at a redshift $z_{ls} = 10 - 1000$ (see Kaiser and Stebbins 1984). In §II I give a more complete calculation of the anisotropy due to an infinite straight string. The formalism for calculating the anisotropy around an object in Minkowski space due to its internal and bulk motion is derived in §III. In §IV I apply this formalism to a spherical cluster of galaxies in order to compare these results with and to extend the work of Birkinshaw and Gull (1982). A review of how a loop of string in Minkowski space moves is given in §V. Certain properties of the anisotropy around a loop which may

be calculated analytically are considered in §VI. In §VII I discuss the anisotropy around a very simple loop geometry which may be calculated analytically. The results of numerical calculation of the anisotropy around more complicated loop configurations are presented in §VIII. I leave the application of the methods developed here to putting constraints on the parameters of string models to a later paper. I only note here that there are at present large theoretical uncertainties in the number density of loops present in the matter era. Thus, at present, no definitive constraints could be determined in any case. In §IX I compare the results obtained here with those of Brandenberger, Albrecht, and Turok (1986). Finally §X contains a summary.

The contents of this paper is only a small part of the program required to determine the full nature of microwave anisotropy produced by cosmic strings. The anisotropy produced at the surface of last scattering bears further study, as do contributions to the Sachs-Wolfe integral from later times. Calculations of the anisotropy due to superhorizon strings requires a formalism appropriate to an expanding universe. Finally we should apply these results to an ensemble of string configurations and model as realistically as possible past and proposed microwave anisotropy experiments.

II. ANISOTROPY FROM AN INFINITE STRAIGHT STRING

Previous calculations of anisotropy of the MBR due to moving objects have been performed by "the method of moving lenses". If a finite object produces a gravitational field which is sufficiently constant in its own rest frame then, in that rest frame, one may consider that object as a lens that does not change the energy of photons passing by it, but only their direction. From this change in direction one may calculate the change in energy in the rest-frame of an observer. The result in the limit of small angle deflections is

$$\frac{\Delta E_O}{E_O} = \varphi \frac{\mathbf{v} \cdot (\hat{\mathbf{l}}_L \times \hat{\mathbf{k}}_L)}{1 + \mathbf{v} \cdot \hat{\mathbf{k}}_L} \tag{2.1}$$

where E_O refers to the energy in the observer frame, $\hat{\mathbf{k}}_L$ is the unit propagation vector of the photon in the lens frame, $\mathbf{v}$ is the velocity of the lens in the observer frame or minus the velocity of the observer in the lens frame, φ is the angle of deflection (assumed $\ll 1$) in the lens frame, and $\hat{\mathbf{l}}_L$ is the unit vector in the lens frame about which the photon direction vector is rotated (in the right-hand rule sense). If, as is relevant for strings, $\hat{\mathbf{l}}_L \cdot \mathbf{v} = 0$, then equation (2.1) may be rewritten

$$\frac{\Delta E_O}{E_O} = \varphi \gamma \hat{\mathbf{k}}_O \cdot (\mathbf{v} \times \hat{\mathbf{l}}_L) \qquad \gamma = (1 - |\mathbf{v}|^2)^{-\frac{1}{2}}. \tag{2.2}$$

where $\hat{\mathbf{k}}_O$ is the unit vector in the direction of propagation of the photon in the observer frame. If, in the observer frame, the lens is backlit by a uniform blackbody background, such as the MBR, then the temperature pattern is given by

$$\frac{\Delta T}{T} = \frac{\Delta E}{E}. \tag{2.3}$$

These equations have been applied to galaxy clusters by Birkinshaw and Gull (1983), who unfortunately used a form of equation (2.3) incorrect by a factor of 2 when calculating the temperature pattern (see §III). In this paper I use the fractional change in temperature and the fractional change in energy interchangeably.

The application of equation (2.1) to an infinite string is somewhat tricky because the geometry around a long straight string in vacuum does not asymptotically approach Minkowski space far from the string. The energy of a photon is not an absolute property of the photon but rather a relation between the photon and the observer. In particular, the velocity of the observer must be specified in addition to his location in spacetime. The energy boost discussed in the previous section refers to the change in energy of a photon as observed by a global "rest frame", i.e a time-like 4-vector field on the spacetime, u^α, satisfying $u^\alpha u_\alpha = -1$ (I shall throughout this paper use metrics with signatures $[-,+,+,+]$). The energy of the photon is then given by $-k^\alpha u_\alpha$ where k^α is the momentum 4-vector of the photon.

Here I shall describe a procedure for specifying the rest frame, u^α in the spacetime of a moving infinite straight string. The procedure used is not the only reasonable procedure, and other reasonable procedures do lead to different results! The ambiguity is not resolvable because the spacetime is not asymptotically Minkowski. I also warn the reader that in what follows I shall always only keep terms to first order in $\tilde{\mu}$ and not include higher order terms. Consider a coordinate system (t,x,y,z) such that an infinite string is located along the z-axis. If the metric were Minkowski then the Lorentz frames boosted in directions orthogonal to the z-axis would be given by

$$u^\alpha(\mathbf{x},t) = \gamma(1,\beta\cos(\theta)\cos(\chi),\beta\sin(\theta)\cos(\chi),\sin(\chi)) \qquad \gamma = (1-\beta^2)^{-\frac{1}{2}}.$$

However the spacetime around a string is not Minkowski, the linearized metric may be written (Vilenkin 1981)

$$g_{\mu\nu} = \eta_{\mu\nu} + h_{\mu\nu} \qquad \eta_{\mu\nu} \equiv \mathrm{diag}(-1,1,1,1) \qquad h_{\mu\nu} = -8\pi\tilde{\mu}\ln\left(\frac{r}{r_0}\right)\mathrm{diag}(0,1,1,0) \quad (2.4)$$

where $r^2 = x^2 + y^2$ and r_0 is arbitrary. This metric is invariant to Lorentz boosts along the string, so we may without loss of generality only consider rest frames moving orthogonally to the string. An obvious analog to the u^α given above, but one which will satisfy $u^\alpha u_\alpha = -1$ in this case, is

$$u^\alpha = \gamma\left(1, \frac{\beta\cos\theta}{\sqrt{g_{11}}}, \frac{\beta\sin\theta}{\sqrt{g_{22}}}, 0\right), \quad (2.5)$$

where I have assumed $\chi = 0$ so the velocity is perpendicular to the string. As noted by Vilenkin (1981) the metric simplifies to the Minkowski form, $\bar{g}_{\mu\nu} = \eta_{\mu\nu}$, if one makes the coordinate transformation

$$\bar{t} = t \quad \bar{x} = x + 4\tilde{\mu}\left((1-\ln(r/r_0))x + \phi\bar{y}\right) \quad \bar{y} = y + 4\tilde{\mu}\left((1-\ln(r/r_0))y - \phi\bar{x}\right) \quad \bar{z} = z \quad (2.6)$$

where $\phi(x,y)$ is defined by $x = r\cos\phi$ and $y = r\sin\phi$ and will be restricted to be in the range $(-\pi,\pi)$. However, whereas the coordinates x and y can take any value, the coordinates $\bar{x}$ and

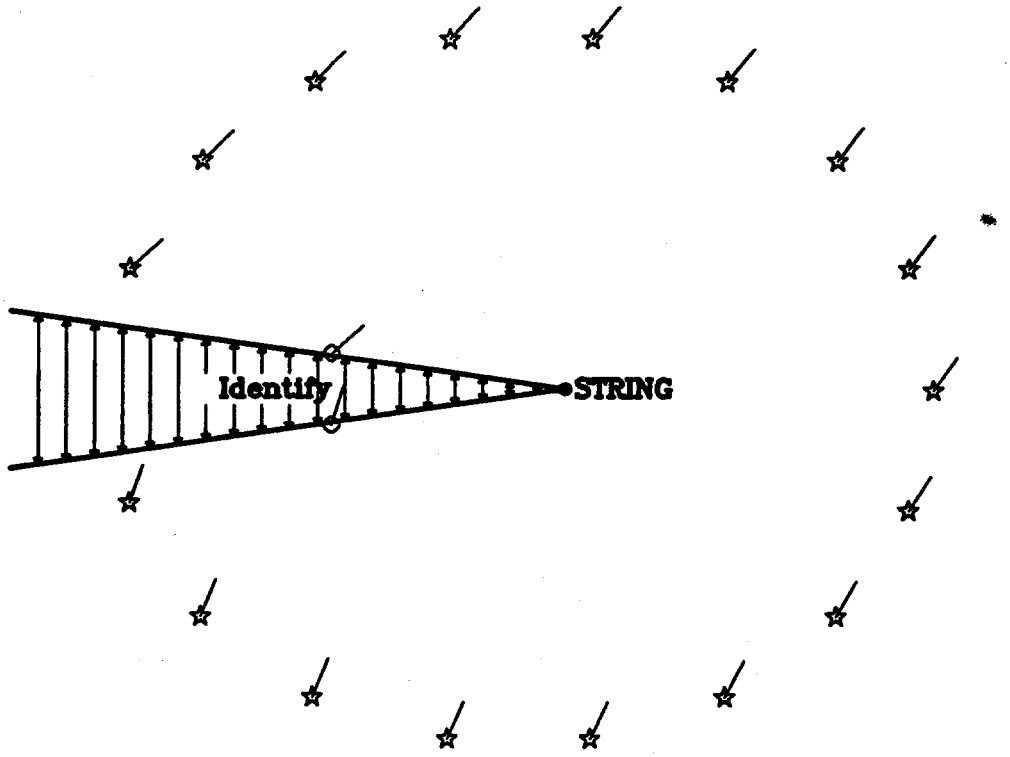

FIGURE 1: Static geometry around an infinite, straight string. Shown here is the $\bar{x}$-$\bar{y}$ plane (see text) is a slice perpendicular to the string. Except at the vertex, which is the string, the geometry is flat. In the text a particular global rest frame moving with respect to the string is defined in analogy with a Lorentz frame in Minkowski space. In this frame the string can be considered to be moving. The circles on the two identified points, representing an observer, and the stars, representing distant emitters of light, are moving with this rest frame. Lines protruding from these symbols indicate their velocities with respect to the coordinate frame. If all the emitters were to emit light with the same temperature then the observer would see different temperatures in different directions due to the differing directions of velocities of the emitters in different directions. The temperature pattern is given by eq. (2.8). The exact pattern depends the choice of global rest frames, and there are other reasonable choices besides the one given here. However, all reasonable choices will give the same value for the temperature jump in the direction of the string. The opening angle of the missing wedge, and thus the string mass parameter, is greatly exaggerated (by a factor $\sim 10^5$).

$\bar{y}$ must satisfy $|\bar{y}| \geq -4\pi\tilde{\mu}\bar{x}$ if $\bar{x} < 0$. The two hyperplanes $\bar{y} = \pm 4\pi\tilde{\mu}\bar{x}$ for $\bar{x} < 0$ are identified. Thus the $\bar{x} - \bar{y}$ plane has a conical geometry with a deficit angle $8\pi\tilde{\mu}$ which is illustrated in Figure 1. One consequence of the conical geometry is that if one were to parallel transport a velocity vector *around* the string and back to the original point the resultant vector will have its $\bar{x} - \bar{y}$ component rotated by an angle $8\pi\tilde{\mu}$. The fact that this remains true even if the path remains arbitrarily far from the string indicates that the spacetime is not asymptotically Minkowski.

In the new coordinates the 4-vector field (2.5) becomes

$$\bar{u}^\alpha = \gamma\left(1, \beta\cos\left(\theta - 4\tilde{\mu}\bar{\phi}\right), \beta\sin\left(\theta - 4\tilde{\mu}\bar{\phi}\right), 0\right) \tag{2.7}$$

where $\bar{\phi}$ is defined by $\bar{x} = \bar{r}\cos\bar{\phi}$ and $\bar{y} = \bar{r}\cos\bar{\phi}$, $\bar{r}^2 = \bar{x}^2 + \bar{y}^2$, and $\bar{\phi} \in (-\pi + 4\pi\tilde{\mu}, \pi + 4\pi\tilde{\mu})$. Now imagine we put an observer at the two identified points $(\bar{t}_o, -\bar{x}_o, \pm 4\pi\tilde{\mu}\,\bar{x}_o, 0)$ moving

with $\bar{u}^\alpha$ and suppose he measures the energy of photons emitted by a particle moving with $\bar{u}^\alpha$ with coordinates $(\bar{t}_e, \bar{x}_e, \bar{y}_e, \bar{z}_e)$ with $\bar{t}_e$ such that all the photons arrive at the same time. Furthermore, assume that all these emitters emit photons with the same energy, E_E, in their rest frame. In the limit of infinite distance to the emitters, the difference in the energy observed from that emitted is given by

$$\frac{E_O - E_E}{E_E} = -\varepsilon 4\tilde{\mu}\beta \cos\bar{\psi}_e \left(\bar{\phi}_e \frac{\sin(\theta - \bar{\phi}_e)}{1 + \beta\cos(\theta - \bar{\phi}_e)\cos\bar{\psi}_e} + \pi \frac{\sin\theta}{1 - \beta\cos\theta\cos\bar{\psi}_e} \right) \qquad (2.8)$$

where

$$\varepsilon = \begin{cases} +1 & \bar{\phi}_e > -4\pi\tilde{\mu} \\ -1 & \bar{\phi}_e < 4\pi\tilde{\mu} \end{cases}, \qquad \sin\bar{\psi}_e = \frac{\bar{z}_e}{\sqrt{\bar{x}_e^2 + \bar{y}_e^2 + \bar{z}_e^2}} \qquad \bar{\psi}_e \in \left(-\frac{\pi}{2}, \frac{\pi}{2}\right),$$

and $\bar{\phi}_e$ is the $\bar{\phi}$ coordinate of the emitter. The ranges of $\bar{\phi}_e$ for the two values of ε overlap due to lensing. The observer will see two images of the same emitter if $\bar{\phi}_e \in (-4\pi\tilde{\mu}, +4\pi\tilde{\mu})$, and the energy of the photons from the two images will be different as indicated above. There is thus a discontinuity in the energy of photons across the image of the string. There is no such discontinuity in the opposite direction near $\bar{\phi}_e = \pm\pi$. I stress that the angles used in equation (2.8) are as measured in frame of the string and bear no simple relation to the angles in the sky of the observer at a fixed time, except in special cases.

Photons which pass much closer to the string than the distance of the string to the observer have $\bar{\phi}_e \ll 1$ and

$$\frac{E_E - E_O}{E_E} \approx -4\pi\tilde{\mu}\varepsilon \frac{\beta\sin\theta\cos\bar{\psi}_e}{1 - \beta\cos\theta\cos\bar{\psi}_e} . \qquad (2.9)$$

Note that the form of equation (2.9) is exactly what we would expect from (2.1) if $\hat{\mathbf{l}}_L$ is along the string and the photon deflects an angle $4\pi\tilde{\mu}$ toward the string as it passes by the string. As noted above there is a discontinuous jump between the energy boost for photons going above and below the string. This discontinuity was discovered by Kaiser and Stebbins (1983) in the case $\theta = \bar{\psi}_e = 0$ and was predicted independently, although not calculated, in Gott (1983). Since the velocity of the string is always perpendicular to the length of the string, equation (2.2) applies to strings. It is clear from equation (2.2) that the maximal discontinuity occurs when $\mathbf{v}$, $\hat{\mathbf{k}}_O$, and $\hat{\mathbf{l}}_L$ are all perpendicular and is

$$\max\left|\frac{E_+ - E_-}{E}\right| = 8\pi\tilde{\mu}\beta\gamma. \qquad (2.10)$$

The choice of geometry analyzed by Kaiser and Stebbins (1983) ($\mathbf{v}$, $\hat{\mathbf{k}}_L$, and $\hat{\mathbf{l}}_L$ all perpendicular) was unfortunate because the discontinuity in the case studied is a factor of γ less than the maximal discontinuity. This might have lead one to believe that the maximal anisotropy was proportional to β and not $\beta\gamma$. In §VI I will show that the discontinuity given by equation (2.2) is correct for strings that are not straight as well. This has already been shown by Vachaspati (1987) in the case of certain types of waves on an infinite string. From now on this paper will deal with loops and not infinite strings. For the case of loops the spacetime will be asymptotically Minkowski, and there will be no ambiguities in the definition of asymptotic rest frames.

III. PHOTON BOOST IN MINKOWSKI SPACE

If there is no rest frame in which the gravitational fields are sufficiently constant then the method of moving lenses cannot be used and a more general approach must be taken. Here I will present the first order change in energy of a photon due to the gravitational field of any object of finite extent which only slightly perturbs Minkowski space along the photon trajectory. Before proceeding I will say a few words about choice of general relativistic gauge. As is well known, gauge freedom (i.e. freedom to choose coordinates) in general relativity may lead to difficulty in giving a physical interpretation to results of calculations in general relativity. However, in what follows the subject of general relativistic gauge will not play a crucial role. The calculations are done in the "radiation gauge" in which equation (3.6) is satisfied. In this gauge the metric deviation must satisfy certain gauge conditions (see Weinberg 1972), but these are not mentioned in this paper. The reason I choose this gauge is that the Green function for the initial value problem is particularly simple in this gauge. The reason I do not need the gauge conditions is that I only use gravitational fields as derived from the Green function and these fields automatically satisfy the gauge conditions. As is well known, the radiation gauge, while removing some gauge freedom does not remove all of it. However, the choice of outgoing modes and asymptotic flatness does. Clearly there is no ambiguity in equation (3.7) below. Finally, as I am only calculating the change in the energy of a photon as measured by observers at asymptotic infinity, and, since there is no ambiguity in setting up an asymptotic rest frame, there is no problem in interpreting the energy shifts derived. The physical system of a string is rather unusual in general relativity. The weak field approximation is a very good one for strings, but the slow motion approximation is not. Most objects that are of interest to relativists are held together by gravity. Therefore, if they are to remain as one object while moving relativistically, the gravitational fields must be strong. Strings, of course, are not held together by gravity and thus may have weak gravitational fields as well as relativistic internal motions.

I now proceed with the calculation of the boost of a photon passing near a string. There are differing sign conventions in general relativity, I shall use the notation of Weinberg (1972) in which, for example, the Minkowski metric is $\eta_{\mu\nu} = \mathrm{diag}(-1,1,1,1)$. The equation of motion of a photon in an arbitrary spacetime geometry is the geodesic equation,

$$\frac{d}{d\lambda}p^\alpha + \Gamma^\alpha_{\beta\gamma}p^\beta p^\gamma = 0 \qquad p^\alpha \equiv \frac{dx^\alpha}{d\lambda}, \tag{3.1}$$

with the restriction $p^\alpha p_\alpha = 0$ (remember that $\frac{d}{d\lambda}p^\alpha p_\alpha = 0$ follows from the geodesic equation). In equation (3.1) p^α is taken to be the photon's 4-momentum, and the arbitrary multiplicative constant usually associated with the affine parameter, λ, is specified by this requirement. I take the geometry to be only slightly perturbed from Minkowski space, i.e. $g_{\mu\nu} = \eta_{\mu\nu} + h_{\mu\nu}$ with $h_{\mu\nu} \ll 1$. To zeroth order in perturbations from Minkowski space ($h_{\alpha\beta} = 0$, $\Gamma^\alpha_{\beta\gamma} = 0$) one may easily solve equation (3.1) obtaining

$$\mathbf{x} = \mathbf{x}_0 + \hat{\mathbf{k}}t \qquad \lambda = \frac{t}{E} \qquad |\hat{\mathbf{k}}| = 1 \qquad p^i = E\,k^i \qquad \text{and} \qquad p^0 = E. \tag{3.2}$$

Here $\hat{\mathbf{k}} = k^i$ is the direction of motion of the photon and E is the energy of the photon as measured in the coordinate frame. The component of $\mathbf{x}_0$ parallel to $\hat{\mathbf{k}}$ determines the time at

which the photon arrives at very distant observers in the $\hat{\mathbf{k}}$ direction. The components of $\mathbf{x}_0$ perpendicular to $\hat{\mathbf{k}}$ tell us the photon's position on the sky of the observer. We are interested in the first order change in the energy of the photon (as measured in the coordinate frame) due to $h_{\alpha\beta}$, keeping the initial energy fixed. This will be given by $p^0(\lambda)$ for which the first order geodesic equation is

$$\frac{d}{d\lambda}p^0 = \frac{1}{2}(2h_{0\beta,\gamma} - h_{\beta\gamma,0})p^\beta p^\gamma = \frac{1}{2}\dot{h}_{00}p^0p^0 + h_{00,i}p^0p^i + h_{0i,j}p^ip^j - \frac{1}{2}\dot{h}_{ij}p^ip^j,$$

since

$$\Gamma^0_{\beta\gamma} = -\frac{1}{2}(h_{0\beta,\gamma} + h_{0\gamma,\beta} - h_{\beta\gamma,0}) + O(h^2_{\alpha\beta}).$$

To first order in $h_{\alpha\beta}$ we may substitute the unperturbed values of $x^\alpha(\lambda)$, $p^\alpha(\lambda)$, and λ. Thus we see that the first order geodesic equation for p^0 (as for all other components) is not coupled to the other first order equations and may be trivially integrated. The result is

$$\frac{p^0(t) - E}{E} \cong \int_{-\infty}^{t}\left[\frac{1}{2}\dot{h}_{00}(\mathbf{x},t) + \hat{\mathbf{k}}\cdot\nabla h_{00}(\mathbf{x},t) + \hat{\mathbf{k}}\cdot\nabla h_{0i}(\mathbf{x},t)k^i - \frac{1}{2}\dot{h}_{ij}(\mathbf{x},t)k^ik^j\right]_{\mathbf{x}=\hat{\mathbf{k}}t} dt. \tag{3.3}$$

Assuming the the gravitational field goes to zero at spatial infinity, one may integrate by parts to obtain an expression for $\Delta E \equiv p^0(+\infty) - p^0(-\infty)$ which just depends on the time derivative of the gravitational fields:

$$\frac{\Delta E}{E} \cong -\int_{-\infty}^{+\infty}\left[\frac{1}{2}\dot{h}_{00}(\mathbf{x}_0 + \hat{\mathbf{k}}t, t) + \dot{h}_{0i}(\mathbf{x}_0 + \hat{\mathbf{k}}t, t)k^i + \frac{1}{2}\dot{h}_{ij}(\mathbf{x}_0 + \hat{\mathbf{k}}t, t)k^ik^j\right]dt. \tag{3.4}$$

Since $h_{\alpha\beta}$ vanishes at spatial infinity, the value of ΔE is the difference between the energy measured in the coordinate frame (which is not perturbed) long after and long before the photon passes through the region in which Minkowski space is perturbed.

It will be convenient to consider the source of the gravitational field to consist of individual particles, labeled by p, each following separate trajectories, $\mathbf{r}^p(t)$. The Ricci tensor may be then be written $R_{\alpha\beta}(\mathbf{x},t) = \sum_p R^p_{\alpha\beta}(t)\delta^{(3)}(\mathbf{x} - \mathbf{r}^p(t))$. To keep the equations compact I use the function

$$\bar{\mathbf{r}}^p(t) \equiv \mathbf{r}^p(t) - \mathbf{x}_0 \tag{3.5}$$

rather than $\mathbf{r}^p(t)$. Since the individual particles will not be constrained to conserve either energy or momentum they may individually contribute monopole or dipole radiation in linearized gravity, although the sum of the gravitational fields from all particles should not. Thus many of our intermediate results will be unphysical. In fact, since monopole radiation will produce a divergence of the final photon energy, many of our intermediate results will be divergent! Einstein's equations linearized in Minkowski space may be written as the wave equation after a suitable choice of gauge (Weinberg 1972),

$$(\nabla^2 - \frac{\partial^2}{\partial t^2})h_{\alpha\beta} = -2R_{\alpha\beta}. \tag{3.6}$$

The Green function solution is

$$h_{\alpha\beta}(\mathbf{x},t) = \frac{2}{4\pi}\int\int \frac{R_{\alpha\beta}(\mathbf{x}',t')\delta(t-t'-|\mathbf{x}-\mathbf{x}'|)}{|\mathbf{x}-\mathbf{x}'|}\,d^3\mathbf{x}'\,dt'. \tag{3.7}$$

The gravitational field from a single particle is thus

$$\begin{aligned} h^p_{\alpha\beta}(\mathbf{x},t) =& \frac{1}{2\pi}\int_{-\infty}^{+\infty} \frac{\delta(t-t'-|\mathbf{x}-\mathbf{r}^p(t')|)R^p_{\alpha\beta}(t')}{|\mathbf{x}-\mathbf{r}^p(t')|}\,dt' \\ =& -\frac{1}{2\pi}\frac{R^p_{\alpha\beta}(\tilde{t}'^p)}{|\mathbf{x}-\mathbf{r}^p(\tilde{t}'^p)| - \dot{\mathbf{r}}^p\cdot(\mathbf{x}-\mathbf{r}^p(\tilde{t}'^p))} \end{aligned} \tag{3.8}$$

where $\tilde{t}'^p = \tilde{t}'^p(\mathbf{x},t)$ is implicitly defined by $t-\tilde{t}'^p = |\mathbf{x}-\mathbf{r}^p(\tilde{t}'^p)|$, and I have used

$$\frac{\partial}{\partial t'}\left[t-t'-|\mathbf{x}-\mathbf{r}^p(t')|\right] = \frac{|\mathbf{x}-\mathbf{r}^p(t')| - \dot{\mathbf{r}}^p\cdot(\mathbf{x}-\mathbf{r}^p(t'))}{|\mathbf{x}-\mathbf{r}^p(t')|} = -\left(\frac{\partial\tilde{t}'^p}{\partial t}\right)^{-1}. \tag{3.9}$$

The time derivative of the gravitational field is then

$$\begin{aligned} 2\pi\,\dot{h}^p_{\alpha\beta}(\mathbf{x},t) =& -\frac{\dot{R}^p_{\alpha\beta}(\tilde{t}'^p)|\mathbf{x}-\mathbf{r}^p(\tilde{t}'^p)|}{[|\mathbf{x}-\mathbf{r}^p(\tilde{t}'^p)| - \dot{\mathbf{r}}^p(\tilde{t}'^p)\cdot(\mathbf{x}-\mathbf{r}^p(\tilde{t}'^p))]^2} \\ & - R^p_{\alpha\beta}(\tilde{t}'^p)\frac{|\mathbf{x}-\mathbf{r}^p(\tilde{t}'^p)|\left\{\bar{\mathbf{r}}^p(\tilde{t}'^p)\cdot(\mathbf{x}-\mathbf{r}^p(\tilde{t}'^p)) - |\dot{\mathbf{r}}^p(\tilde{t}'^p)|^2\right\} + \dot{\mathbf{r}}^p(\tilde{t}'^p)\cdot(\mathbf{x}-\mathbf{r}^p(\tilde{t}'^p))}{[|\mathbf{x}-\mathbf{r}^p(\tilde{t}'^p)| - \dot{\mathbf{r}}^p(\tilde{t}'^p)\cdot(\mathbf{x}-\mathbf{r}^p(\tilde{t}'^p))]^3} \end{aligned} \tag{3.10}$$

One must now integrate this time derivative along the photon trajectory,

$$\begin{aligned} \int_{-\infty}^{+\infty}\dot{h}^p_{\alpha\beta}(\mathbf{x}_0+\hat{\mathbf{k}}t,t)dt =& -\frac{1}{2\pi}\int_{-\infty}^{+\infty}\left\{\frac{\dot{R}^p_{\alpha\beta}(\bar{t}'^p)|\hat{\mathbf{k}}t-\bar{\mathbf{r}}^p(\bar{t}'^p)|}{[|\hat{\mathbf{k}}t-\bar{\mathbf{r}}^p(\bar{t}'^p)| - \dot{\mathbf{r}}^p(\bar{t}'^p)\cdot(\hat{\mathbf{k}}t-\bar{\mathbf{r}}^p(\bar{t}'^p))]^2}\right. \\ & \left. + R^p_{\alpha\beta}(\bar{t}'^p)\frac{|\hat{\mathbf{k}}t-\bar{\mathbf{r}}^p(\bar{t}'^p)|\{\bar{\mathbf{r}}^p(\bar{t}'^p)\cdot(\hat{\mathbf{k}}t-\bar{\mathbf{r}}^p(\bar{t}'^p)) - |\dot{\mathbf{r}}^p(\bar{t}'^p)|^2\} + \dot{\mathbf{r}}^p(\bar{t}'^p)\cdot(\hat{\mathbf{k}}t-\bar{\mathbf{r}}^p(\bar{t}'^p))}{[|\hat{\mathbf{k}}t-\bar{\mathbf{r}}^p(\bar{t}'^p)| - \dot{\mathbf{r}}^p(\bar{t}'^p)\cdot(\hat{\mathbf{k}}t-\bar{\mathbf{r}}^p(\bar{t}'^p))]^3}\right\}dt \end{aligned} \tag{3.11}$$

Here $\bar{t}'^p = \bar{t}'^p(t)$ is implicitly defined by $t-\bar{t}'^p = |\hat{\mathbf{k}}t-\bar{\mathbf{r}}^p(\bar{t}'^p)|$. It is more convenient to integrate with respect to the particle's coordinate time, $\bar{t}'^p$, rather than the light ray's coordinate time, t. As long as the trajectory of the particle remains timelike, ($|\dot{\mathbf{r}}^p| < 1$), $\bar{t}'^p(t)$ maps the interval $t\in(-\infty,+\infty)$ monotonically onto $t\in(-\infty, t'^p_{\max})$, where $t'^p_{\max}$ is implicitly and uniquely defined by

$$t'^p_{\max} = \hat{\mathbf{k}}\cdot\bar{\mathbf{r}}^p(t'^p_{\max}). \tag{3.12}$$

The inverse function of $\bar{t}'^p(t)$ is

$$\bar{t}^p(t') = \frac{1}{2}\left[\frac{t'^2-|\bar{\mathbf{r}}^p(t')|^2}{t'-\hat{\mathbf{k}}\cdot\bar{\mathbf{r}}^p(t')}\right]. \tag{3.13}$$

The integral now reads

$$\int_{-\infty}^{+\infty} \dot{h}^p_{\alpha\beta}(\hat{\mathbf{k}}t,t)dt =$$

$$-\frac{1}{2\pi}\int_{-\infty}^{t'^p_{max}} \left\{ \frac{\dot{R}^p_{\alpha\beta}(t')|\hat{\mathbf{k}}\bar{t}^p - \bar{\mathbf{r}}^p(t')|}{[|\hat{\mathbf{k}}\bar{t}^p - \bar{\mathbf{r}}^p(t')| - \dot{\mathbf{r}}^p(t')\cdot(\hat{\mathbf{k}}\bar{t}^p - \bar{\mathbf{r}}^p(t'))][|\hat{\mathbf{k}}\bar{t}^p - \bar{\mathbf{r}}^p(t')| - \hat{\mathbf{k}}\cdot(\hat{\mathbf{k}}\bar{t}^p - \bar{\mathbf{r}}^p(t'))]} \right.$$

$$\left. + R^p_{\alpha\beta}(t')\frac{[|\hat{\mathbf{k}}\bar{t}^p - \bar{\mathbf{r}}^p(t')|\{\bar{\mathbf{r}}^p(t')\cdot(\hat{\mathbf{k}}\bar{t}^p - \bar{\mathbf{r}}^p(t')) - |\dot{\mathbf{r}}^p(t')|^2\} + \dot{\mathbf{r}}^p(t')\cdot(\hat{\mathbf{k}}\bar{t}^p - \bar{\mathbf{r}}^p(t'))]}{[|\hat{\mathbf{k}}\bar{t}^p - \bar{\mathbf{r}}^p(t')| - \dot{\mathbf{r}}^p(t')\cdot(\hat{\mathbf{k}}\bar{t}^p - \bar{\mathbf{r}}^p(t'))]^2[|\hat{\mathbf{k}}\bar{t}^p - \bar{\mathbf{r}}^p(t')| - \hat{\mathbf{k}}\cdot(\hat{\mathbf{k}}\bar{t}^p - \bar{\mathbf{r}}^p(t'))]} \right\} dt' \tag{3.14}$$

Using Einstein's equations, $R_{\alpha\beta} = 8\pi(T_{\alpha\beta} - \frac{1}{2}g_{\alpha\beta}T^{\mu}{}_{\mu})$ and equation (3.4), after some algebra we obtain

$$\frac{\Delta E}{E} \cong -4\sum_p \int_{-\infty}^{t'^p_{max}} \left(2\frac{S^p}{D} - \frac{B}{\bar{\mathbf{r}}^p\cdot\hat{\mathbf{k}} - t'}\frac{\partial}{\partial t'}\left(\frac{S^p}{D}\right)\right) dt' \tag{3.15}$$

where

$$B(t') = (\bar{\mathbf{r}}^p\cdot\hat{\mathbf{k}} - t')^2 + R, \qquad R(t') = |\bar{\mathbf{r}}^p|^2 - (\bar{\mathbf{r}}^p\cdot\hat{\mathbf{k}})^2,$$

$$D(t') = (\bar{\mathbf{r}}^p\cdot\hat{\mathbf{k}} - t')^2(1 + \dot{\mathbf{r}}^p\cdot\hat{\mathbf{k}}) + (\bar{\mathbf{r}}^p\cdot\hat{\mathbf{k}} - t')\dot{R} + (1 - \dot{\mathbf{r}}^p\cdot\hat{\mathbf{k}})R,$$

$$S^p(t') = \left[\frac{1}{2}T^p_{00}(t') + T^p_{0i}(t')k^i + \frac{1}{2}T^p_{ij}(t')k^ik^j\right].$$

Here $T^p_{\alpha\beta}$ is the contribution to the stress-energy tensor from a single particle, i.e. $T_{\alpha\beta}(\mathbf{x},t) = \sum_p T^p_{\alpha\beta}(t)\delta^{(3)}(\mathbf{x} - \mathbf{r}^p(t))$. One might be tempted to integrate equatioon (3.15) by parts, however one cannot because the integrand is divergent at the upper time limit when $t' = \hat{\mathbf{k}}\cdot\bar{\mathbf{r}}^p(t')$. In fact, the integral is divergent at the upper time limit, as shall now be discussed.

Singular Behavior of Formalism

Before proceeding, it is important to check the integral (3.15) for any singular behavior. The terms in the numerator clearly remain finite for $t' \in (-\infty, t'^p_{max})$. A singularity may also occur if one of the factors in the denominators becomes zero. First consider the term D. One may always choose the spacetime coordinate system such that the particle in consideration at the time in consideration is at the origin and at $t' = 0$. For $\mathbf{r}^p(0) = 0$ and $t' = 0$, D takes the simple form

$$D = (1 - \dot{\mathbf{r}}^p\cdot\hat{\mathbf{k}})|\mathbf{x}_0|^2 + 2\mathbf{x}_0\cdot\hat{\mathbf{k}}\,\dot{\mathbf{r}}^p\cdot\mathbf{x}_0 \qquad \mathbf{x}_0\cdot\hat{\mathbf{k}} \le 0 \tag{3.16}$$

where the inequality comes from the requirement that $t'^p_{max} \ge 0$. One can show that D is positive definite for $\mathbf{x}_0 \neq 0$ and $|\dot{\mathbf{r}}^p| < 1$. In the case of strings there will be particles which momentarily approach the speed of light and may cause D to approach zero. The physical reason for the singularity is as follows. If a particle approaches the speed of light, it will become nearly resonant with gravity wave modes moving in approximately the same direction as the particle's motion. This particle will excite these modes, creating a pulse of strong gravity waves moving outward at the speed of light in the direction in which the particle was moving when it approached the speed of light. The condition $D = 0$ for $\mathbf{x}_0 \neq 0$ is just the condition that the photon trajectory intersects the trajectory of such a pulse.

However, as we shall see, these pulses have no effect on the anisotropy. The other case when $D = 0$ is when $\mathbf{x_0} = 0$. If $\mathbf{x_0} = 0$, then the $t' = t'^p_{\max}$ and the light trajectory has intersected the particle in question. This is an extremely degenerate case to which the formalism should not be applied. It will be shown in §V that photons passing on either side of a string are perfectly well behaved no matter how close they approach the string. The divergence at $\mathbf{x_0} = 0$ has no physical significance.

The other term in the denominator, $\bar{\mathbf{r}}^p \cdot \hat{\mathbf{k}} - t'$, will become zero at the upper time limit, $t' = t'^p_{\max}$, and this will, in general, cause the integral, equation (3.15), to be divergent at the upper time limit. If we denote the integrand of equation (3.15) by $-I^0_p(t')$, then the divergence is apparent:

$$\lim_{t' \to t'^p_{\max}} I^0_p(t') = \frac{1}{(t'^p_{\max} - t')} \left[\frac{\partial}{\partial t'} \left(\frac{S^p}{1 - \hat{\mathbf{k}} \cdot \dot{\mathbf{r}}^p} \right) \right]_{t' = t'^p_{\max}} . \tag{3.17}$$

If the derivative term is nonzero, which will generally be true, the integral will be logarithmically divergent. This is an artifact of dividing the full spacetime stress-energy tensor into unphysical pieces. The sum of the contributions from all particles will not be divergent as long as energy-momentum is locally conserved. Using the asymptotic form (3.18) in the integral (3.15) and transforming the variable of integration back to photon time as in equation (3.13), we obtain for the asymptotic contribution from all particles

$$\begin{aligned} \lim_{\substack{t_- \to +\infty \\ t_+ \to +\infty}} \sum_p \int_{\bar{t}'^p(t_-)}^{\bar{t}'^p(t_+)} I^0_p(t')\, dt' &= \lim_{\substack{t_- \to +\infty \\ t_+ \to +\infty}} I^0_p(\bar{t}'^p(t)) \frac{d\bar{t}'^p(t)}{dt}\, dt \\ &= \sum_p \frac{1}{1 - \hat{\mathbf{k}} \cdot \dot{\mathbf{r}}^p(t'^p_{\max})} \left[\frac{\partial}{\partial t'} \left(\frac{S^p}{1 - \hat{\mathbf{k}} \cdot \dot{\mathbf{r}}^p} \right) \right]_{t' = t'^p_{\max}} \int_{t_-}^{t_+} \frac{dt}{t}. \end{aligned} \tag{3.18}$$

However, the divergence is, in fact, not real because the coefficient is zero. It is shown in the appendix that

$$\sum_p \frac{1}{1 - \hat{\mathbf{k}} \cdot \dot{\mathbf{r}}^p(t'^p_{\max})} \left[\frac{\partial}{\partial t'} \left(\frac{S^p}{1 - \hat{\mathbf{k}} \cdot \dot{\mathbf{r}}^p} \right) \right]_{t' = t'^p_{\max}} = 0. \tag{3.19}$$

However, this singular behavior will lead to problems in numerical integrations of equation (3.15) if one does not take special steps to avoid it. We may use this equation to transform equation (3.15) to a more useful form.

One should also examine the behavior of the integral for large negative times. To do this one must specify how a particle's trajectory behaves for large negative times. We shall require that the particles acceleration, $\ddot{\mathbf{r}}^p$, and the particles velocity, $\dot{\mathbf{r}}^p$, remain bounded. For our applications these conditions will be satisfied. It is not, however, reasonable to require that the particles position remains bounded. In general, one expects that the center of mass of the object to which the particle is attached will undergo ballistic motion. Thus one may write the particles trajectory as

$$\bar{\mathbf{r}}^p(t') = \bar{\bar{\mathbf{r}}}^p(t') + \bar{\mathbf{v}} t', \tag{3.20}$$

where $\bar{\mathbf{r}}^p(t')$ is bounded. Evaluating the leading terms for large t', one finds that

$$\lim_{t'\to-\infty} I_p^0(t') = \frac{1}{(1-\bar{\mathbf{v}}\cdot\hat{\mathbf{k}})t'}\frac{\partial}{\partial t'}\left(\frac{S^p}{1+\hat{\mathbf{n}}\cdot\dot{\mathbf{r}}^p}\right) \tag{3.21}$$

where

$$\hat{\mathbf{n}} = \frac{(1-|\bar{\mathbf{v}}|^2)\hat{\mathbf{k}} - 2(1-\bar{\mathbf{v}}\cdot\hat{\mathbf{k}})\bar{\mathbf{v}}}{1+|\bar{\mathbf{v}}|^2 - 2\bar{\mathbf{v}}\cdot\hat{\mathbf{k}}} \qquad |\hat{\mathbf{n}}| = 1\,.$$

As long as the term in parentheses remains bounded, its time derivative will have zero time average and the integral will converge. The denominator will remain positive (i.e. nonzero) as long as $|\bar{\mathbf{v}}| < 1$ and $|\hat{\mathbf{k}}\cdot\dot{\mathbf{r}}^p| < 1$. The first condition will be satisfied for all reasonable objects. The second condition is the condition that the particle not move at the speed of light directly at the observer. For the case of strings this is not an impossibility. However, it will happen only for a set of measure zero of string configurations, and this possibility will thus be ignored.

Simplification

Keeping the foregoing discussion in mind we may still proceed to try to simplify equation (3.15). In order to manipulate the equations sensibly, we must regulate the divergence in some way. The method we shall use is to evaluate the integral at an upper time limit, less than $t'^p_{\max}$. In particular, we will take this upper time limit to be $t'^p_{\max} - \epsilon_p$. After invoking equation (3.19), we will be able take the limit $\epsilon_p \to 0$ and obtain a finite result. Integrating equation (3.15) by parts we obtain

$$\frac{\Delta E}{E} \cong 4\sum_p \left\{ \int_{-\infty}^{t'^p_{\max}-\epsilon_p} \left(\frac{(\bar{\mathbf{r}}^p\cdot\hat{\mathbf{k}} - t')\dot{B} + (1-\dot{\mathbf{r}}^p\cdot\hat{\mathbf{k}})B}{(\bar{\mathbf{r}}^p\cdot\hat{\mathbf{k}} - t')^2} + 2 \right) \frac{S^p}{D}\,dt' \right.$$
$$\left. - \left[\frac{S^p B}{(\bar{\mathbf{r}}^p\cdot\hat{\mathbf{k}} - t')D} \right]_{t'=t'^p_{\max}-\epsilon_p} \right\}. \tag{3.22}$$

One may derive the following identities:

$$(\bar{\mathbf{r}}^p\cdot\hat{\mathbf{k}} - t')\left(\dot{B} - 2(\bar{\mathbf{r}}^p\cdot\hat{\mathbf{k}} - t')\right) + (1-\dot{\mathbf{r}}^p\cdot\hat{\mathbf{k}})B = D,$$

$$\int_{-\infty}^{t'^p_{\max}-\epsilon_p} \frac{S^p}{(\bar{\mathbf{r}}^p\cdot\hat{\mathbf{k}} - t')^2}\,dt' = \left[\frac{S^p}{(\bar{\mathbf{r}}^p\cdot\hat{\mathbf{k}} - t')(1-\dot{\mathbf{r}}^p\cdot\hat{\mathbf{k}})} \right]_{t'=t'^p_{\max}-\epsilon_p}$$
$$- \int_{-\infty}^{t'^p_{\max}-\epsilon_p} \frac{1}{\bar{\mathbf{r}}^p\cdot\hat{\mathbf{k}} - t'}\frac{\partial}{\partial t'}\left(\frac{S^p}{1-\dot{\mathbf{r}}^p\cdot\hat{\mathbf{k}}}\right) dt',$$

and

$$\lim_{\epsilon_p\to 0}\left[\frac{S^p}{\bar{\mathbf{r}}^p\cdot\hat{\mathbf{k}} - t'}\left(\frac{B}{D} - \frac{1}{1-\dot{\mathbf{r}}^p\cdot\hat{\mathbf{k}}}\right)\right]_{t'=t'^p_{\max}-\epsilon_p} = \left[\frac{\dot{R}}{R}\frac{S^p}{(1-\dot{\mathbf{r}}^p\cdot\hat{\mathbf{k}})^2}\right]_{t'=t'^p_{\max}}. \tag{3.23}$$

Combining with equation (3.21) one obtains

$$\frac{\Delta E}{E} \cong 4 \sum_p \left\{ \int_{-\infty}^{t'^p_{\max}} I_p(t')\, dt' + C_p \right\} \tag{3.24}$$

where

$$I_p = \frac{1}{\mathbf{r}^p \cdot \hat{\mathbf{k}} - t'} \frac{\partial}{\partial t'} \left(\frac{S^p}{1 - \dot{\mathbf{r}}^p \cdot \hat{\mathbf{k}}} \right) \qquad C_p = \left[\frac{\dot{R}}{R} \frac{S^p}{(1 - \dot{\mathbf{r}}^p \cdot \hat{\mathbf{k}})^2} \right]_{t' = t'^p_{\max}} . \tag{3.25}$$

The term, I_p, carries the divergence and is clearly of the form (3.17). We are thus assured that the divergences cancel. Note that the term D has disappeared from the denominator. Thus the equation for the photon boost does not diverge when $D = 0$. Therefore we should not expect particularly strong boosts when a photon passes through the pulses described above.

A surprising result is that not only is the sum of the integrals of I_p finite, but it is zero. We now proceed with proof. Consider the variable $\mathbf{x}_0$ which, along with $\hat{\mathbf{k}}$, identifies the photon in consideration. We may break $\mathbf{x}_0$ into a piece parallel to $\hat{\mathbf{k}}$ and perpendicular to $\hat{\mathbf{k}}$:

$$\mathbf{x}_0 = \mathbf{x}_\perp - \hat{\mathbf{k}} r \qquad \mathbf{x}_\perp \cdot \hat{\mathbf{k}} = 0. \tag{3.26}$$

From equation (3.12) we see that $t'^p_{\max}$ only depends on r and not on $\mathbf{x}_\perp$. For the purposes of the proof we shall consider photon trajectories with different value of r than that of the photon for which we are calculating the boost. To avoid confusion we shall denote these values by $\hat{r}$. For each value of $\hat{r}$ and for each particle p there will be value t', call it $\hat{t}'_p$, defined analogous to $t'^p_{\max}$, i.e.

$$\hat{t}'_p(\hat{r}): \qquad \hat{\mathbf{k}} \cdot \mathbf{r}^p(\hat{t}'_p) + \hat{r} - \hat{t}'_p = 0. \tag{3.27}$$

For the particle trajectories we will consider, the function $\hat{t}'_p(\hat{r})$ is a smooth, one-to-one mapping of the interval $(-\infty, +\infty)$ in $\hat{r}$ to the interval $(-\infty, +\infty)$ in t'. It is possible, therefore, to change the variable of integration in equation (3.24) from t' to $\hat{r}$. It will be convenient to choose, for each particle p, $\epsilon_p = \hat{t}'_p(r - \hat{\epsilon})$. Performing the change of variables, we obtain

$$\begin{aligned} \sum_p \int_{-\infty}^{\hat{t}'_p(r-\hat{\epsilon})} & \frac{1}{\mathbf{r}^p \cdot \hat{\mathbf{k}} - t'} \frac{\partial}{\partial t'} \left(\frac{S^p}{1 - \dot{\mathbf{r}}^p \cdot \hat{\mathbf{k}}} \right) dt' \\ & = \int_{-\infty}^{r-\hat{\epsilon}} \frac{1}{r - \hat{r}} \sum_p \left[\frac{1}{1 - \dot{\mathbf{r}}^p \cdot \hat{\mathbf{k}}} \frac{\partial}{\partial t'} \left(\frac{S^p}{1 - \dot{\mathbf{r}}^p \cdot \hat{\mathbf{k}}} \right) \right]_{\hat{t}'_p(\hat{r})} d\hat{r}. \end{aligned} \tag{3.28}$$

Clearly equation (3.19) is valid with $t'^p_{\max}$ replaced with $\hat{t}'_p(\hat{r})$ because $\hat{t}'_p(\hat{r})$ is just $t'^p_{\max}$ for a different photon. Thus the sum inside the integral of equation (3.27) is zero and the integral is thus zero for all values of $\hat{\epsilon}$. We thus conclude

$$\sum_p \int_{-\infty}^{t'^p_{\max}} I_p(t')\, dt' = \lim_{\hat{\epsilon} \to 0} \sum_p \int_{-\infty}^{\hat{t}'_p(r-\hat{\epsilon})} I_p(t')\, dt' = 0. \tag{3.29}$$

This greatly simplifies the equation for the photon boost. Equation (3.24) becomes

$$\frac{\Delta E}{E} \cong 4 \sum_p \left[\frac{\dot{R}}{R} \frac{S^p}{(1 - \dot{\mathbf{r}}^p \cdot \hat{\mathbf{k}})^2} \right]_{t' = t'^p_{\max}} \tag{3.30}$$

which is our final result.

The result that the total photon boost only depends on what the loop is doing at $t'^p_{\max}$ may seem somewhat mysterious. Clearly the photon has been in causal contact with the perturber for all times previous to that, and it is not obvious why the effects of the gravitational fields produced by the perturber at all times previous to $t'^p_{\max}$ should exactly cancel. One heuristic argument for the cancellation goes as follows. The direction of propagation from the perturber to a point on the photon trajectory is not parallel to the direction of the photon, $\hat{\mathbf{k}}$, for all perturber times $t' < t'^p_{\max}$. If one considers the gravitational field propagating in a given direction as a sum of sinusoidal waves traveling at the speed of light, it is clear that the time-averaged contribution to the integral (3.4) is zero unless the wave is traveling in exactly the same direction as the photon. In the latter case the integral is formally infinite. If we take the limits of integration of equation (3.4) to be finite then each sine wave will contribute a boundary term to the integral. As the sine-waves must conspire to add up to zero net gravitational field far from the loop, it is not surprising that the boundary terms from all waves not parallel to $\hat{\mathbf{k}}$ should add to zero. It is also not surprising that the formally infinite integral from the waves emitted at $t'^p_{\max}$ and propagating parallel to $\hat{\mathbf{k}}$ should conspire to sum to a finite result when one includes the phase coherence required to cause the gravitational fields to fall off at infinity. This heuristic argument as well as the derivation of equation (3.29) suggests that the exact cancellations are a consequence of taking the observer to be infinitely far from the perturbing object. If we were to take the observer to be a finite distance from the perturber, then we would expect a contribution to the photon boost due to the motions of the perturber before $t'^p_{\max}$. The contribution should be small for the observer much further from the perturber than its size and should be of increasing importance as the observer approaches the perturber.

Limitations of Formalism

Let us review what the meaning of equation (3.30). We have calculated the change in energy of a photon from passing through the gravitational field of an isolated, localized source imbedded in Minkowski space. Since the only source of gravitational fields is a finite isolated source the spacetime is asymptotically flat and we may choose an asymptotic rest frames without any ambiguity. The energy shift is measured with respect to a particular asymptotic rest frame. The shift being the difference in energy between when it is measured at $t \to -\infty$ before it passes the source, and the energy when it is measured at $t \to +\infty$ after it passes by the source. The fields were calculated using linearized general relativity in the radiation gauge, and the energy shift was calculated in the linearized sense of equation (3.2). This energy shift is expressed in terms of the stress-energy tensor of the source. The stress-energy tensor was decomposed into the sum of the stress-energy tensor of individual particles which must not move superluminally. In addition, they must never move at the speed of light in the direction of the motion of the photon. To obtain the total energy shift one must sum over

all the particles of the source. We have eliminated contributions to the photon boost which are zero when local conservation of energy-momentum is exactly obeyed but which diverge when this condition is not satisfied. This will allow easier numerical implementation of the formalism where one would inevitably represent a continuum of particles by a finite number, which could not obey local energy-momentum conservation.

We would like to apply this formula to the comparison of the energy shifts of photons arriving at an observer at the same time from different directions. The gravitational field will cause different photons to experience different time delays. Corrections to ΔE which include these time delays are second order in $|h^2_{\alpha\beta}|$ but this does not necessarily mean that they are small. If an object of size R produces a gravitational field of size h, then photons passing through the object will experience time delays of $\sim hR/c$ and the minimum time in which the object as a whole can change is $\sim R/c$. If $h \ll 1$, as has been assumed, then it is probably valid to ignore time delays. It is not, however, valid to ignore time delays when the object possesses rapidly changing substructure which significantly effects some of the photons or if the light source is rapidly varying. For the purposes of this paper time delays are unimportant. The temperature of microwave background is not rapidly varying, and for most string configurations we expect no rapidly varying substructure.

Another limitation of calculating only the linearized energy shift is that we have ignored the change in direction of the photon trajectory as it passes the object. The change in angle of photons will typically be $\sim h$ and will vary by this amount over the projected surface of the object. Thus we have typically miscalculated the photon position by an amount $\sim hR \ll R$. Unless the object has very small substructure, we have only miscalculated the gravitational field that the photon experiences by a small amount. Also, if the source of photons had structure on angular scales $\sim h$ times the angular size of the source, and if this structure could be confused with the photon boosts calculated here, then we would not be able to predict the observed pattern on the sky using this formalism. For the case at hand, these deflections are of little importance. Strings do have very small substructure in the sense that the width of strings are microscopic while their lengths are astronomical. Furthermore, there is a significant discontinuity in boost across the projection of a length of string on the sky. The effect of the fact that we have ignored such deflections is that the calculated image of the temperature pattern on the sky will have the angular position of these discontinuities misplaced by of order $h\,(\sim 10^{-6})$ times the angular size of the loop. This error is of no observational significance. Furthermore, we do not expect the microwave background to have significant substructure on very small scales due to the smoothing effect of the surface of last scattering. Thus errors due to deflections are insignificant. In summary, it is quite reasonable to ignore second order corrections to ΔE when calculating anisotropy due to strings.

Application to Sky Maps

Given that most loops that we would observe existed at redshifts much greater than unity, what significance does the above calculation of boosts in Minkowski space have to predictions of anisotropies we could observe? We must first restrict ourselves to loops that were much smaller than the horizon when the microwave photons we see passed by the loop. Furthermore, the impact parameter of the photons with respect to the loop must be smaller than the horizon size at that time. If these two conditions are satisfied, then the

gravitational fields used are approximately correct, and thus the above calculation of the boost of the photon as they passed by the loop will be approximately valid. Ignoring other inhomogeneities, the effect of the cosmology after the photon passes near the loop will just be to redshift all photons equally. SInce this will not change the relative fractional differences in the energy of the photons, it will not change the pattern of anisotropy. We may just linearly superpose anisotropies due to other inhomogeneities to the anisotropy calculated for the loop in question. To reiterate, the anisotropy calculated here is valid for subhorizon loops and only for photons passing much closer than a horizon distance to the loop. A generalization of the method derived here to a cosmological setting is being developed at present by Veeraraghavan, Stebbins, and Silk (1987) for the purpose of calculating the anisotropy due to superhorizon strings.

The photons satisfying the conditions stated in the previous paragraph will all have been moving approximately parallel when they passed the loop. Thus all the photons we see will have approximately the same $\hat{\mathbf{k}}$. The parameter $\mathbf{x}_0$ determines both the position in our sky of the light trajectory and the time at which this light trajectory arrives at our detector. If we decompose $\mathbf{x}_0$ as in equation (3.26) then the term $\mathbf{x}_\perp$ determines where in the sky the photon will come from and τ determines at which time we receive it. In particular, the larger τ is the later we receive the photon.

IV. ANISOTROPY FROM MOVING CLUSTERS

As a check of the results of the previous section we may apply it to a simple example, the case of a single particle moving in a straight line at constant velocity. The temperature fluctuation pattern in the MBR from a moving point mass has already been calculated by Birkinshaw and Gull (1983) using the moving lens technique. We take the trajectory to be $\mathbf{r}^p(t) = \mathbf{r}_0 + \vec{\beta}t$. One may always redefine t so that $(\mathbf{r}_0 - \mathbf{x}_0) \cdot \hat{\mathbf{k}} = 0$. In this case $\mathbf{x}_0 - \mathbf{r}_0$ will be the apparent position of the particle as seen by a sufficiently distant observer situated along the photon trajectory at the time when the photon reaches the observer. The stress-energy tensor of the particle will be $T^p_{00} = \gamma m$, $T^p_{0i} = -\gamma m \beta_i$, and $T^p_{ij} = \gamma m \beta_i \beta_j$; where $\gamma = (1-\beta^2)^{-\frac{1}{2}}$ and m is the mass of the particle. Using the above notation (3.30) becomes

$$\frac{\Delta T}{T} = \frac{\Delta E}{E} = -4m\gamma \frac{\vec{\beta} \cdot (\mathbf{x}_0 - \mathbf{r}_0)}{|\mathbf{x}_0 - \mathbf{r}_0|^2}, \tag{4.1}$$

which is the result of Birkinshaw and Gull (1983). Birkinshaw and Gull derived this result to estimate the anisotropy produced by the transverse motion of clusters of galaxies. We pause here to extend this analysis to somewhat more realistic models of the mass distribution of clusters than the constant density sphere used in Birkinshaw and Gull (1983). First note that for a collection of moving particles the anisotropy pattern on the sky is just the sum of the patterns of the individual particles. For systems with nonrelativistic velocity dispersion the motion of the individual particles are well represented by their ballistic motion at the time the observed photons pass through them, in which case the pattern for an individual particle is just given by equation (4.1). So for a collection of particles

$$\frac{\Delta T}{T} = \sum_p -4m\gamma \frac{\vec{\beta} \cdot (\mathbf{x}_0 - \mathbf{r}^p_0)}{|\mathbf{x}_0 - \mathbf{r}^p_0|^2}. \tag{4.2}$$

For a continuous, spherically symmetric density distribution moving uniformly with a transverse velocity $v_\perp$ equation (4.2) becomes

$$\frac{\Delta T}{T} = -\frac{4GM_{\rm proj}(r_{\rm proj})v_\perp}{c^3 r_{\rm proj}}\cos(\phi), \tag{4.3}$$

where $M_{\rm proj}(r_{\rm proj})$ is the projected mass within the projected radius, $r_{\rm proj}$, and ϕ is the angle between $\mathbf{v}_\perp$ and $\mathbf{r}_{\rm proj}$. If one models a cluster as having a spherical density profile $\rho(r) = \rho_0(1 + (r/r_{\rm core})^2)^{-\varsigma}$, and define $v_c \equiv \sqrt{G\rho_0 r_{\rm core}^2}$ then (4.3) becomes

$$\frac{\Delta T}{T} = -1.3\times 10^{-7}\frac{v_c^2 v_\perp}{(10^3\,{\rm km/sec})^3}\frac{\Gamma(\varsigma-\frac{1}{2})}{\Gamma(\frac{3}{2}-\varsigma)\Gamma(\varsigma)}\frac{r_{\rm core}}{r_{\rm proj}}\left[\left(1+\frac{r_{\rm proj}^2}{r_{\rm core}^2}\right)^{\frac{3}{2}-\varsigma}-1\right]\cos(\phi). \tag{4.4}$$

We see that for reasonable cluster parameters this effect is far from being detectable at present and is, in any case, liable to be swamped by the Sunyaev-Zel'dovich effect even for clusters with small gas content. This is true whether or not one accepts the very large cluster peculiar velocities reported by Burstein *et al.* (1986) or by Collins, Joseph, and Robertson (1986).

I conclude this section with a word of caution concerning applying the above equations to a system acting under Newtonian gravity. It was just shown that this formalism may give infinite results if the condition of local energy-momentum conservation is not satisfied. However, in Newtonian gravity the particles interact through "action at a distance", and energy-momentum is not *locally* conserved. Therefore including the gravitational acceleration of the particles in their trajectories will in general lead to divergent results. In fact, it is not even consistent to include the gravitational acceleration to the particles in calculating the boost to a photon because such terms are second order in G, and we have ignored other terms of the same order in deriving the above equations. In short, one must not include the contribution of gravitational fields to the time derivatives of the stress-energy tensor when using the formalism developed in this paper.

V. COSMIC STRINGS IN MINKOWSKI SPACE

The dynamics of strings was developed in Goddard *et al.* (1973) and applied to cosmic strings in Kibble and Turok (1982) and many later works. If one ignores the internal dynamics of the matter fields which make a cosmic string, the interaction of the string with the matter around it, and the backreaction of gravity on the string; then the equations of motion of a cosmic string in Minkowski space can be solved exactly. All of these approximations will be very good for cosmic strings long after the epoch in which they are formed. The dynamical theory of cosmic strings is identical to the classical theory of "massless strings" which was developed over a decade ago to try to explain the mass spectrum of mesons. While the "massless strings" of particle physics may have free ends, this cannot happen for cosmic strings produced in phase transitions. We will restrict our attention to string loops in this paper saving the discussion of infinite strings in an expanding universe for a later paper. We may describe the motion of a string in a specific Minkowski rest frame by a function $\mathbf{r}(\sigma, t)$ which gives the position of a specific point on the string, labeled by σ, at time t. We have much freedom in how we assign σ to points on the string at different times. An especially nice

choice is one where particles of constant σ move perpendicular to the length of the string. i.e.

$$\dot{\mathbf{r}} \cdot \mathbf{r}' = 0. \tag{5.1}$$

Here $'$ denotes differentiation with respect to σ and $\dot{}$ denotes differentiation with respect to time. It was shown by Goddard *et al.* (1973) that equation (5.1) is consistent with the further requirement

$$|\dot{\mathbf{r}}|^2 + |\mathbf{r}'|^2 = 1, \tag{5.2}$$

and that with this choice of σ the equations of motion take the simple form:

$$\ddot{\mathbf{r}} - \mathbf{r}'' = 0. \tag{5.3}$$

If the velocity of the closed loop perpendicular to its length is everywhere initially less than the speed of light, i.e. $|\dot{\mathbf{r}}| < 1$, then it will remain so except on a discrete set of points on the σ-t plane where the velocity will equal the speed of light. While tachyonic solutions to string dynamics exist they will not be important for cosmic strings. The above prescription determines σ up to a constant and we will further specify that around the loop it varies from 0 to L where

$$L \equiv \oint d\sigma = \oint (1 - |\dot{\mathbf{r}}|^2)^{-\frac{1}{2}} |d\mathbf{r}|, \tag{5.4}$$

which is constant in time. Equation (5.3) may be solved easily. With the requirement for a loop that $\mathbf{r}(\sigma, t)$ be periodic in σ, the most general solution is

$$\mathbf{r}(\sigma, t) = \frac{1}{2}\left(\mathbf{a}_+(t+\sigma) + \mathbf{a}_-(t-\sigma)\right) + \bar{\mathbf{v}}t \tag{5.5}$$

where $\mathbf{a}_+$ and $\mathbf{a}_-$ are periodic functions with period L. The $\bar{\mathbf{v}}$ term represents the center of mass motion of the string and apart from this secular term the string evolution is periodic. From equation (5.5) it is clear that the motion of the particles of constant σ have orbits which are periodic with period L. However, in the string center-of-mass frame, equation (5.5) tells us that $\mathbf{r}(\sigma, t) = \mathbf{r}(\sigma + L/2, t + L/2)$ so the actual period of the string configuration is $L/2$ and may be smaller in certain special cases. Equations (5.1) and (5.2) place additional constraints on $\mathbf{a}_+$ and $\mathbf{a}_-$. In the center-of-mass frame we define

$$\begin{aligned} \mathbf{A}_+(u) &\equiv \frac{d}{du}\mathbf{a}_+(u) \\ \mathbf{A}_-(w) &\equiv \frac{d}{dw}\mathbf{a}_-(w) \end{aligned} \qquad (\bar{\mathbf{v}} = 0). \tag{5.6}$$

Equations (5.1) and (5.2) then require

$$|\mathbf{A}_+(u)| = |\mathbf{A}_-(w)| = 1, \tag{5.7}$$

so $\mathbf{A}_+$ and $\mathbf{A}_-$ are parameterized closed curves on the unit 2-sphere with period L. The only other constraint on these curves comes from the requirement that $\mathbf{a}_+$ and $\mathbf{a}_-$ are periodic. This tells us that

$$\oint \mathbf{A}_+(u)\, du = \oint \mathbf{A}_-(w)\, dw = 0. \tag{5.8}$$

When two pieces of string collide, they will either pass through each other or else the four segments meeting at the point of collision will become connected differently than initially. This latter process is called intercommutation. During intercommutation the string will not obey the equation of motion (5.3) but it will both before and after. If, for example, a loop intercommutes with itself, then it will become two loops, and the functions (5.7) describing the two loops will be different from, but related to, the functions describing the initial loop.

The curve in real space traced out by a string will be smooth so long as $|\mathbf{r}'| > 0$ or equivalently $|\dot{\mathbf{r}}| < 1$. This condition will be violated at points where $\mathbf{A}_+(t+\sigma) = \mathbf{A}_-(t-\sigma)$ which will occur once each period for each time the curves traced out by $\mathbf{A}_+$ and $\mathbf{A}_-$ on the 2-sphere intersect. These points will correspond to times and places where the curve traced out by the string has a cusp. The velocity of the string at the tip of the cusp will equal the speed of light. Since two curves on a 2-sphere will generically intersect an even number of times, there will generically be an even number of cusps in the string trajectory per period. These cusps are structurally stable in the sense that no small perturbation of the string configuration will cause them to disappear. Some consequences of these cusps have been discussed by Turok (1982).

In the case of cusps a string which is initially smooth will momentarily develop a pointed cusp which then disappears. However, strings may also have nonsmooth features that do not disappear. Such features will appear when two strings intercommute. During intercommutation $\mathbf{r}'$ will become discontinuous, and the string will therefore have a sharp bend in it. This sharp bend will immediately break into two sharp bends which will propagate in either direction along the string at the speed of light. These two bends propagating at the speed of light are called "kinks". In terms of the description of string trajectories given here the two kinks correspond to the discontinuities in the two functions $\mathbf{A}_+$ and $\mathbf{A}_-$ which are created as one piece of a string is connected to another during the intercommutation process. It is expected that these discontinuities smooth themselves out due to gravitational backreaction and dynamical friction from the surrounding medium but how rapidly this will occur is not known. These discontinuities will, in a probabilistic sense, tend to lead to cusps which are very small in size (Thompson 1987, Albrecht, Copeland, and Turok 1987). Since string intercommutation is a common occurence, kinks and their associated cusps will be numerous on long strings and loops.

The string trajectory near a kink may be expressed as follows. We may choose the coordinates $\mathbf{x}$, t, and σ such that at $t = 0$ the kink passes through the point $\mathbf{x} = 0$ in space and through the string segment $\sigma = 0$. Expanding the string trajectory to first nonvanishing order in σ and t we obtain

$$\mathbf{r}(\sigma,t) = \begin{cases} \mathbf{r}_1'\sigma + \dot{\mathbf{r}}_1 t + \ldots & \sigma > v_\sigma t + \ldots \\ \mathbf{r}_2'\sigma + \dot{\mathbf{r}}_2 t + \ldots & \sigma < v_\sigma t + \ldots \end{cases}, \tag{5.9}$$

In order that the two segments remain connected requires that

$$(\mathbf{r}_1' - \mathbf{r}_2')v_\sigma = -(\dot{\mathbf{r}}_1 - \dot{\mathbf{r}}_2) \tag{5.10}$$

The gauge conditions (5.1) and (5.2) lead to obvious conditions on $\dot{\mathbf{r}}_1$, $\dot{\mathbf{r}}_2$, $\mathbf{r}_1'$, and $\mathbf{r}_2'$. The equation of motion (5.3) leads to the condition

$$(\mathbf{r}_1' - \mathbf{r}_2') = -(\dot{\mathbf{r}}_1 - \dot{\mathbf{r}}_2)v_\sigma. \tag{5.11}$$

Combining (5.9) and (5.10) we obtain $v_\sigma = \pm 1$ corresponding to either a left-moving or right-moving kink, which gives

$$\dot{\mathbf{r}}_1 \pm \mathbf{r}_1' = \dot{\mathbf{r}}_2 \pm \mathbf{r}_2' = \hat{\mathbf{v}}_{\mathbf{kink}} \quad \text{for} \quad v_\sigma = \pm 1 \quad \text{and} \quad |\hat{\mathbf{v}}_{\mathbf{kink}}| = 1. \tag{5.12}$$

One may easily check that $\mathbf{v}_{\mathbf{kink}}$ is the velocity of the kink, which thus moves at the speed of light.

We shall need particular string configurations in order to explore the anisotropy from loops. A particularly nice class of loops was discovered in Turok (1984) and is given by

$$\mathbf{A}_+(u) = \cos u\,\hat{\mathbf{x}} + \cos\phi\,\sin u\,\hat{\mathbf{y}} + \sin\phi\,\cos u\hat{\mathbf{z}}$$

$$\mathbf{A}_-(w) = (\alpha\cos w + (1-\alpha)\cos 3w)\,\hat{\mathbf{x}} + (\alpha\sin w + (1-\alpha)\sin 3w)\,\hat{\mathbf{y}} + 2\,(\alpha(1-\alpha))^{\frac{1}{2}}\,\sin w\hat{\mathbf{z}} \tag{5.13}$$

where $\alpha \in [0,1]$ and $\phi \in [-\pi, +\pi]$. Of course, one may perform a rotation, a translation, a reflection, or any combination of these to also obtain valid string configuration. One may also Lorentz boost the above to obtain valid sting configurations. However, in the case of a Lorentz boost, one would have to reparameterize the string (i.e. choose a new σ coordinate) if one wished to remain in the gauge given by equations (5.1-2). Some of these configurations do have cusps but none have kinks.

The dynamics of strings does not depend on the mass parameter of the string: $\tilde{\mu}$. However the gravitational field produced by these moving strings will be proportional to $\tilde{\mu}$. The formalism developed in the last section requires the stress-energy tensor of strings. This has been derived by Turok (1984) in terms of the function $\mathbf{r}(\sigma, t)$ discussed above. He obtained

$$T_{\alpha\beta}(\mathbf{x}, t) = \tilde{\mu} \oint \begin{pmatrix} 1 & -\dot{\mathbf{r}} \\ -\dot{\mathbf{r}} & \dot{r}_i\dot{r}_j - r_i'r_j' \end{pmatrix} \delta^{(3)}(\mathbf{x} - \mathbf{r}(\sigma, t))\, d\sigma \tag{5.14}$$

In the previous section we dealt with the gravitational field of individual particles. For strings we will consider the particles to be the points on the strings labeled by constant σ. Thus in place of an index p we have a functional dependence on σ. Sums over p are replaced by integrals over σ. With this change in notation and (5.14) we find

$$S^p(\sigma, t) = \frac{1}{2}\tilde{\mu}\left((1 - \dot{\mathbf{r}}\cdot\hat{\mathbf{k}})^2 - (\mathbf{r}'\cdot\hat{\mathbf{k}})^2\right). \tag{5.15}$$

We may write the equation for the photon boost, (3.30), explicitly

$$\frac{\Delta E}{E} \cong -4\tilde{\mu} \oint \left(\frac{\mathbf{u}\cdot(\mathbf{x}_\perp - \mathbf{r}^{\mathbf{proj}})}{|\mathbf{x}_\perp - \mathbf{r}^{\mathbf{proj}}|^2}\right) d\sigma, \tag{5.16}$$

where

$$\mathbf{r}^{\mathbf{proj}}(\sigma) \equiv \left[\mathbf{r} - (\mathbf{r}\cdot\hat{\mathbf{k}})\hat{\mathbf{k}}\right]_{t'=t'^p_{\max}(\sigma)}$$

and

$$\mathbf{u}(\sigma) \equiv \left[\left(1 - \frac{(\mathbf{r}'\cdot\hat{\mathbf{k}})^2}{(1-\dot{\mathbf{r}}\cdot\hat{\mathbf{k}})^2}\right)\left(\dot{\mathbf{r}} - (\dot{\mathbf{r}}\cdot\hat{\mathbf{k}})\hat{\mathbf{k}}\right)\right]_{t'=t'^p_{\max}}.$$

This expression for the anisotropy pattern at a fixed time is manifestly two-dimensional since the vectors $\mathbf{u}$, $\mathbf{r}^{\rm proj}$, and $\mathbf{x}_\perp$ all lie in the plane perpendicular to $\hat{\mathbf{k}}$. The curve traced by the string on the sky at this fixed time is given by $\mathbf{r}^{\rm proj}(\sigma)$. The expression for the vector $\mathbf{u}(\sigma)$ may be simplified by use of the identity

$$|\mathbf{r}^{\rm proj\,\prime}| \equiv \frac{d}{d\sigma}\mathbf{r}^{\rm proj}(\sigma) = |\mathbf{r}'|\sqrt{1-\frac{(\mathbf{r}_0'\cdot\hat{\mathbf{k}})^2}{(1-\dot{\mathbf{r}}_0\cdot\hat{\mathbf{k}})^2}}, \tag{5.17}$$

which yields

$$\mathbf{u} = |\mathbf{r}^{\rm proj\,\prime}|^2\left[\frac{\dot{\mathbf{r}}-(\dot{\mathbf{r}}\cdot\hat{\mathbf{k}})\hat{\mathbf{k}}}{|\mathbf{r}'|^2}\right]_{t'=t'^{\rm p}_{\rm max}}. \tag{5.18}$$

We caution the reader that $\mathbf{r}^{\rm proj\,\prime}$ is not the projection of $\mathbf{r}'(\sigma, t'^{\rm p}_{\rm max}(\sigma))$ onto the plane perpendicular to $\hat{\mathbf{k}}$. For example, a moving straight ($\mathbf{r}'$ constant) string will appear curved ($\mathbf{r}^{\rm proj\,\prime}$ varying) to an observer due to time-retardation effects.

We stress that these results are specific to the string gauge defined by equations (5.1-2). For a given loop one must perform a one-dimensional integral for each photon one considers. If one wanted a sky map around a loop as seen at a given time, one would perform a two-parameter set of these one-dimensional integrals. Except in very special cases, such as the one discussed in §VII, the integrals cannot be solved in terms of simple functions. Thus, although the problem was simplified considerably in §III, one is still quite far from obtaining results regarding the anisotropy around loops. However, we may use equation (5.16) to be a little more specific about implementing equation (3.30) in the case of strings.

VI. MBR ANISOTROPY FROM LOOPS: NEAR AND FAR

In this section we use equation (5.16) to derive analytic expressions for various aspects of the temperature pattern produced by a cosmic string. We examine the the temperature pattern very near a smooth piece of string, very near a kink, and very near a cusp. We also derive expressions for the temperature pattern very far from a string loop. Ambiguities regarding the total luminosity of a loop are discussed. Finally it is shown that away from the loop the temperature pattern satisfies Laplace's equation in two dimensions. Various consequences of this result are mentioned.

Anisotropy Pattern Near a Smooth Segment of String

The analysis in §II of an infinite straight string suggests that there will be a discontinuous jump in the boost given to a photon passing on either side of a piece of string. The discontinuity for an infinite string is given by equation n(2.2), with $\hat{\mathbf{l}}_{\rm L} \parallel \mathbf{r}'$. The sign is such that the photon will get less energy if it passes "in front" of a moving piece of string and more if it passes "in back". Given that $|\mathbf{r}'| = \gamma^{-1}$, we see that the result of §II is

$$\frac{\Delta T_b - \Delta T_f}{T} = 8\pi\tilde{\mu}\frac{|\dot{\mathbf{r}}\cdot(\mathbf{r}'\times\hat{\mathbf{k}})|}{|\mathbf{r}'|^2}. \tag{6.1}$$

The subscripts b and f stand for photons passing in back of and in front of the moving string respectively. In fact, Vachaspati (1986) has derived equation (6.1) for a broad class

of nonlinear waves on infinite strings for which the full spacetime metric may be written in terms of simple functions. Indeed, it would be surprising if it were not true for all string configurations. We shall derive it below using equation (5.16).

Suppose a piece of string passes the through the point in spacetime $\mathbf{x} = 0$ and $t = 0$. We may choose the parameterization σ so that $\sigma = 0$ at this point. Furthermore let the derivatives of the string trajectory at this point be $\dot{\mathbf{r}}_0$, $\mathbf{r}_0'$, $\dot{\mathbf{r}}_0'$, and $\tilde{\mathbf{r}}_0$. We expand all quantities in σ and $\delta \equiv |\mathbf{x}_\perp|$, the distance of the photon trajectory from the string particle, $\sigma = 0$, at $t = 0$. The function $t'^p_{\rm max}(\sigma)$ may be expanded as

$$t'^p_{\rm max}(\sigma) = \frac{\mathbf{r}_0' \cdot \hat{\mathbf{k}}}{1 - \dot{\mathbf{r}}_0 \cdot \hat{\mathbf{k}}}\sigma + ... \tag{6.2}$$

Expanding $\mathbf{r}^{\rm proj}(\sigma)$ about $\sigma = 0$ we obtain

$$\mathbf{r}^{\rm proj}(\sigma) = \mathbf{r}^{\rm proj\,\prime}{}_0\sigma + ... \qquad \mathbf{r}_0^{\rm proj\,\prime} = \frac{(1 - \dot{\mathbf{r}}_0 \cdot \hat{\mathbf{k}})\mathbf{r}_0' + (\mathbf{r}_0' \cdot \hat{\mathbf{k}})\dot{\mathbf{r}}_0 - (\mathbf{r}_0' \cdot \hat{\mathbf{k}})\hat{\mathbf{k}}}{(1 - \dot{\mathbf{r}}_0 \cdot \hat{\mathbf{k}})}. \tag{6.3}$$

We parameterize the photon trajectories as

$$\mathbf{x}_0 = \mathbf{x}_\perp = \delta(\cos\theta\,\hat{\mathbf{n}}_\parallel + \sin\theta\,\hat{\mathbf{n}}_\perp) \tag{6.4}$$

where

$$\hat{\mathbf{k}}\cdot\hat{\mathbf{n}}_\perp = \hat{\mathbf{k}}\cdot\hat{\mathbf{n}}_\parallel = \hat{\mathbf{n}}_\perp\cdot\hat{\mathbf{n}}_\parallel = \hat{\mathbf{n}}_\perp\cdot\mathbf{r}_0^{\rm proj\,\prime} = 0, \qquad |\hat{\mathbf{n}}_\perp| = |\hat{\mathbf{n}}_\parallel| = 1, \qquad \text{and} \qquad \hat{\mathbf{n}}_\perp\cdot\dot{\mathbf{r}}_0 \geq 0. \tag{6.5}$$

In words, θ is the angle between $\mathbf{x}_\perp$ and $\mathbf{r}_0^{\rm proj\,\prime}$, δ is distance between the photon and the string particle $\sigma = 0$ at $t = 0$, $\hat{\mathbf{n}}_\parallel$ is the unit vector perpendicular to $\hat{\mathbf{k}}$ and parallel to $\mathbf{r}_0^{\rm proj\,\prime}$, and $\hat{\mathbf{n}}_\perp$ is the unit vector perpendicular to both $\hat{\mathbf{k}}$ and $\mathbf{r}_0^{\rm proj\,\prime}$. The sign of $\hat{\mathbf{n}}_\perp$ is determined by the last equation except in the case when $\dot{\mathbf{r}}_0$ has no component perpendicular to both $\hat{\mathbf{k}}$ and $\mathbf{r}_0^{\rm proj\,\prime}$. This ambiguity in sign of $\hat{\mathbf{n}}_\perp$ will not lead to an ambiguity in the temperature pattern. If $\sin\theta > 0$ then the photon passes in front of the moving string, and if $\sin\theta < 0$ then it passes in back. We do not consider the case where the photon passes through the string, i.e. $\sin\theta = 0$. With this notation the integral (5.16) to lowest order in σ and δ may easily be performed. We require that the upper and lower limits of integration be sufficiently small that the Taylor expansions used are good approximations in the interval in between. If we denote the upper and lower limits of the integral by σ^+ and σ^-, respectively, then the answer is

$$\begin{aligned}\frac{\Delta T}{T} = -4\tilde{\mu}\frac{|\mathbf{r}_0^{\rm proj\,\prime}|}{|\mathbf{r}_0'|^2}\Bigg\{&\frac{1}{2}(\dot{\mathbf{r}}_0\cdot\hat{\mathbf{n}}_\parallel)\ln\left[\frac{(|\mathbf{r}_0^{\rm proj\,\prime}|\sigma^+ - \delta\cos\theta|)^2 + \delta^2\sin^2\theta}{(|\mathbf{r}_0^{\rm proj\,\prime}|\sigma^- - \delta\cos\theta|)^2 + \delta^2\sin^2\theta}\right] + \\ &(\dot{\mathbf{r}}_0\cdot\hat{\mathbf{n}}_\perp)\left[\tan^{-1}\left(\frac{|\mathbf{r}_0^{\rm proj\,\prime}|\sigma^+ - \delta\cos\theta}{\delta\sin\theta}\right) - \tan^{-1}\left(\frac{|\mathbf{r}_0^{\rm proj\,\prime}|\sigma^- - \delta\cos\theta}{\delta\sin\theta}\right)\right]\Bigg\}.\end{aligned} \tag{6.6}$$

We are interested in the anisotropy pattern very close to the string and thus take the limits $(\delta/\sigma^+) \to 0_+$ and $(\delta/\sigma^-) \to 0_-$ to obtain

$$\lim_{\delta\to 0}\frac{\Delta E}{E} = -4\tilde{\mu}\frac{|\mathbf{r}_0^{\mathrm{proj}\,\prime}|}{|\mathbf{r}_0'|^2}\left\{(\dot{\mathbf{r}}_0\cdot\hat{\mathbf{n}}_{\parallel})\ln\left|\frac{\sigma^+}{\sigma_-}\right| + \pi(\dot{\mathbf{r}}_0\cdot\hat{\mathbf{n}}_{\perp})\mathrm{sgn}(\sin\theta)\right\}. \tag{6.7}$$

The logarithmic term in equation (6.7) depends on the actual values of the limits chosen. However it does not depend on either δ or θ and is just an additive term for all photons. One can group this term with the contribution of the string far from the point in consideration to the anisotropy at this point. The second term does depend on the photon trajectory but only through the sign of $\sin\theta$. The pattern very near a straight piece of string is thus a constant temperature in front of the string and different temperature in back. The actual temperatures depend on the what the string far from the segment in consideration are doing, but the difference in temperatures depends only on the motion of the this segment. We may simplify equation (6.7) with the following identities:

$$\begin{aligned} &|\mathbf{r}_0^{\mathrm{proj}\,\prime}|(\dot{\mathbf{r}}_0\cdot\hat{\mathbf{n}}_{\perp}) = |\dot{\mathbf{r}}_0\cdot(\mathbf{r}_0^{\mathrm{proj}\,\prime}\times\hat{\mathbf{k}})| = |\dot{\mathbf{r}}_0\cdot(\mathbf{r}_0'\times\hat{\mathbf{k}})|, \\ \text{and}\qquad &|\mathbf{r}_0^{\mathrm{proj}\,\prime}|(\dot{\mathbf{r}}_0\cdot\hat{\mathbf{n}}_{\parallel}) = |\dot{\mathbf{r}}_0\cdot\mathbf{r}_0^{\mathrm{proj}\,\prime}| = \frac{(\mathbf{r}_0'\cdot\hat{\mathbf{k}})(|\dot{\mathbf{r}}_0|^2 - \dot{\mathbf{r}}_0\cdot\hat{\mathbf{k}})}{(1-\dot{\mathbf{r}}_0\cdot\hat{\mathbf{k}})|}, \end{aligned} \tag{6.8}$$

Combining these identities with equation (6.7), one obtains for the temperature jump across the string becomes

$$\frac{\Delta T_b - \Delta T_f}{T} = 8\pi\tilde{\mu}\frac{|\dot{\mathbf{r}}_0\cdot(\mathbf{r}_0'\times\hat{\mathbf{k}})|}{|\mathbf{r}_0'|^2} \tag{6.9}$$

which is identical to (6.1). Thus the moving lens analysis for an infinite straight string in §II faithfully gives the correct formula for temperature jump across any piece of string.

Anisotropy Pattern near a Kink

We parameterize the string near a kink exactly as we did in §V (see eq. 5.9). Without loss of generality we consider a kink moving in the $+\sigma$ direction along the string and will thus take $v_\sigma = +1$ in what follows. As in the previous subsection we expect that the parts of the string very far from the kink may contribute a roughly constant temperature boost to the region near the kink but will otherwise not effect the pattern. We need only consider the temperature pattern at a given time. As the string evolves the temperature pattern around the kink will continue to be of the form described here, but parameters may change. Very near to the kink the string may be approximated by two straight segments: the segment, $\sigma < 0$ (segment 1), corresponding to the string behind the kink, and the segment, $\sigma > 0$ (segment 2), corresponding to the segment into which the kink is moving. For each straight segment we may use the result (6.9), changing the subscript 0 to either 1 or 2 for the two segments and adding the appropriate subscript to the angle θ. Making this change of notation, taking the limits $(\delta/\sigma^+) \to 0_+$ and $(\delta/\sigma^-) \to 0_-$, and using the identities (6.8), we obtain

$$\begin{aligned} \frac{\Delta T}{T} = -4\tilde{\mu}\Bigg[&\left\{\frac{(\mathbf{r}_1'\cdot\hat{\mathbf{k}})(|\dot{\mathbf{r}}_1|^2 - \dot{\mathbf{r}}_1\cdot\hat{\mathbf{k}})}{(1-\dot{\mathbf{r}}_1\cdot\hat{\mathbf{k}})|\mathbf{r}_1'|^2}\ln\left|\frac{\delta}{|\mathbf{r}_1^{\mathrm{proj}\,\prime}|\sigma^-}\right| + \theta_1\frac{|\dot{\mathbf{r}}_1\cdot(\mathbf{r}_1'\times\hat{\mathbf{k}})|}{|\mathbf{r}_1'|^2}\right\} + \\ &\left\{\frac{(\mathbf{r}_2'\cdot\hat{\mathbf{k}})(|\dot{\mathbf{r}}_2|^2 - \dot{\mathbf{r}}_2\cdot\hat{\mathbf{k}})}{(1-\dot{\mathbf{r}}_2\cdot\hat{\mathbf{k}})|\mathbf{r}_2'|^2}\ln\left|\frac{|\mathbf{r}_2^{\mathrm{proj}\,\prime}|\sigma^+}{\delta}\right| + (\pi-\theta_2)\frac{|\dot{\mathbf{r}}_2\cdot(\mathbf{r}_2'\times\hat{\mathbf{k}})|}{|\mathbf{r}_2'|^2}\right\}\Bigg] \end{aligned} \tag{6.10}$$

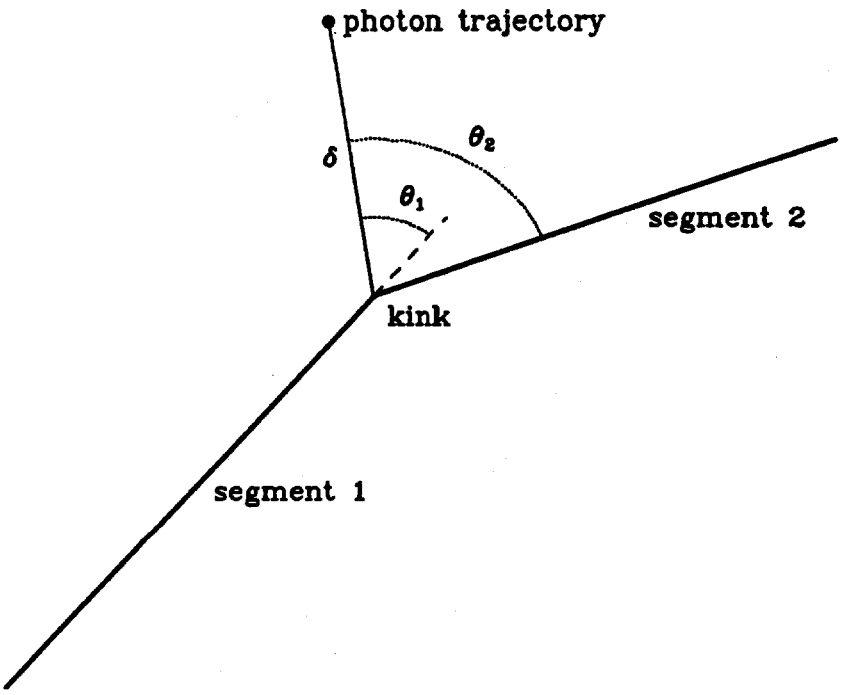

FIGURE 2: Projection on the sky of the string near a kink. The meaning of the parameters δ, θ_1, and θ_2 for a specific photon trajectory is illustrated.

where $\theta_1 \in (-\pi, \pi)$ and $\theta_2 \in (0, 2\pi)$ (see Figure 2). If $\dot{\mathbf{r}}_1 = \dot{\mathbf{r}}_2$ and $\mathbf{r}'_1 = \mathbf{r}'_2$ then $\theta_1 = \theta_2$ and we recover the result for a smooth piece of string, equation (6.9).

As in the previous subsection we may ignore the parts of equation (6.10) which do not depend on the photon trajectory contributing only an additive constant boost to all photons. Equation (6.10) becomes

$$\frac{\Delta T}{T} = -4\tilde{\mu}\left[\left\{\frac{(\mathbf{r}'_2\cdot\hat{\mathbf{k}})(|\dot{\mathbf{r}}_2|^2 - \dot{\mathbf{r}}_2\cdot\hat{\mathbf{k}})}{(1-\dot{\mathbf{r}}_2\cdot\hat{\mathbf{k}})|\mathbf{r}'_2|^2} - \frac{(\mathbf{r}'_1\cdot\hat{\mathbf{k}})(|\dot{\mathbf{r}}_1|^2 - \dot{\mathbf{r}}_1\cdot\hat{\mathbf{k}})}{(1-\dot{\mathbf{r}}_1\cdot\hat{\mathbf{k}})|\mathbf{r}'_1|^2}\right\}\ln|\delta| + \theta_1\frac{|\dot{\mathbf{r}}_1\cdot(\mathbf{r}'_1\times\hat{\mathbf{k}})|}{|\mathbf{r}'_1|^2} + (\pi-\theta_2)\frac{|\dot{\mathbf{r}}_2\cdot(\mathbf{r}'_2\times\hat{\mathbf{k}})|}{|\mathbf{r}'_2|^2}\right]. \tag{6.11}$$

The only relation between the segments 1 and 2 is equation (5.12), and from this we see that the term in brackets in previous equation is not, in general, zero. Thus the pattern of anisotropy around an kink consists of two parts. The first part depends logarithmically on the impact parameter of the photon with respect to the kink. The coefficient of the logarithm may have either sign. Formally as one looks closer and closer to the kink the MBR temperature will diverge, although the divergence is not very strong. Of course, the analysis here is invalid unless $\Delta T/T \ll 1$, and, as noted in §V kinks are expected to smooth themselves out. Formula (6.10) will be valid for smoothed kinks when δ is much larger than the scale of smoothing. This logarithmic term will produce hotspots or coldspots on the MBR.

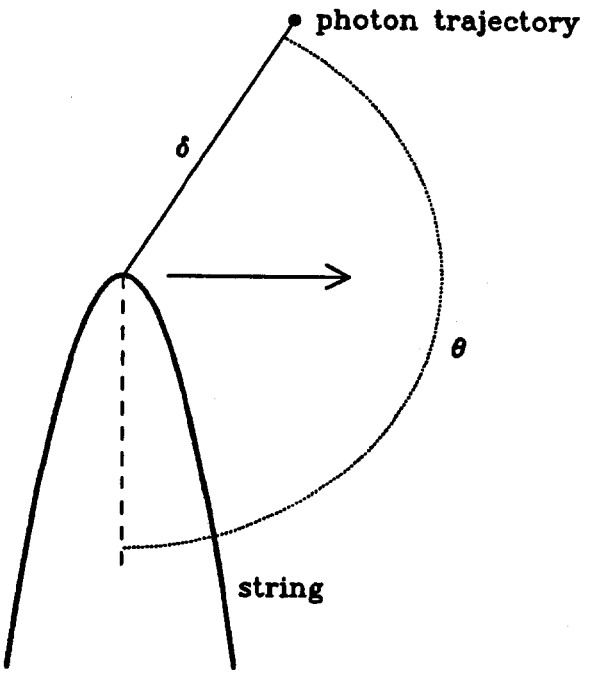

FIGURE 3: Projection on the sky of the string near a piece about to go through or just having gone through a cusp. If we were looking during the time of the cusp, the parabola, which is the string, would collapse to a semiline. The meaning of the parameters δ and θ for a specific photon trajectory is illustrated. The direction of the arrow is the direction of $\mathbf{r}_0^{proj\,\prime}$ (see text).

The last two terms in equation (6.10) describe part of the pattern which depends on the angular position of the photon around the kink and is divided into the contribution from part 1 and part 2 of the string. This is contribution is described in Figure 2. The average boost of the angular part is zero. It is interesting to note that by looking at the pattern of anisotropy around a kink it is impossible to determine which way the kink is moving.

Anisotropy Pattern Near a Cusp

It was mentioned in §IV that loop trajectories will occasionally form cusps where the string will not be smooth. At these isolated points $\mathbf{r}' \to 0$ and $|\dot{\mathbf{r}}| \to 1$. The analysis given above regarding the discontinuity clearly cannot apply in this case because the string is not smooth. However, as we approach the cusp in either space or time the string is smooth, and the discontinuity diverges because the velocity of the string segment approaches the speed of light. Thus we would expect very large anisotropies spatially or temporally near a cusp. In this subsection we perform calculation to determine the pattern of anisotropy near the projection of a cusp on the sky. Using the constraints (4.1-3) the trajectory of a string spatially and temporally close to a cusp can be expanded as

$$\mathbf{r}(\sigma,t') = \hat{\mathbf{m}}t' + \frac{1}{2}\ddot{\mathbf{r}}_0(t'^2+\sigma^2) + \dot{\mathbf{r}}_0'\sigma t' + \ldots \qquad |\hat{\mathbf{m}}| = 1 \quad \ddot{\mathbf{r}}_0\cdot\hat{\mathbf{m}} = 0 \quad \dot{\mathbf{r}}_0'\cdot\hat{\mathbf{m}} = 0, \qquad (6.12)$$

where $\hat{\mathbf{m}}$ is a unit vector in the direction in which the particle at the tip of the cusp moves at the speed of light. I have chosen the coordinates (σ, $\mathbf{x}$, t) such that the cusp occurs at $\mathbf{x} = \sigma = t = 0$. Unlike in the case of a smooth piece of string or a kink the nature of the temperature pattern around a cusp will qualitatively change with the time of observation. Using the notation of equation (3.26), τ tells us the time at which the photons reach us. Observation of the cusp at $\tau < 0$, $\tau = 0$, and $\tau > 0$ correspond to photons which passed the string at times before, during, and after the cusp, respectively. To simplify the equation we use

$$\tilde{\tau} \equiv \frac{\tau}{1 - \hat{\mathbf{m}} \cdot \hat{\mathbf{k}}} \tag{6.13}$$

instead of τ. The function $t'^{p}_{\max}(\sigma)$, expanded to second order in τ and σ is

$$t'^{p}_{\max}(\sigma) = \tilde{\tau} + \frac{(\vec{\mathbf{r}}_0 \cdot \hat{\mathbf{k}})\left(\sigma^2 + \tilde{\tau}^2\right) + 2(\dot{\mathbf{r}}'_0 \cdot \hat{\mathbf{k}})\sigma\tilde{\tau}}{1 - \hat{\mathbf{m}} \cdot \hat{\mathbf{k}}} + O(\tilde{\sigma}^3, \tilde{\sigma}^2\tilde{\tau}, \tilde{\sigma}\tilde{\tau}^2, \tilde{\tau}^3). \tag{6.14}$$

For fixed $\tilde{\tau} \neq 0$ and to second order in σ the curve traced out by the string on the sky, $\mathbf{r}^{\mathrm{proj}}$, is a parabola. When $\tilde{\tau} = 0$, then the string develops a cusp and is not smooth. If we reparameterize the string with

$$\tilde{\sigma}(\tilde{\tau}) \equiv \sigma + \frac{\vec{\mathbf{r}}_0 \cdot \dot{\mathbf{r}}'_0}{|\vec{\mathbf{r}}_0|^2}\tilde{\tau} + O(\tilde{\tau}^2) \tag{6.15}$$

then the string particle on the tip of the parabola has $\tilde{\sigma} = 0$. The curve traced out by the string as a function of $\tilde{\tau}$ is

$$\mathbf{r}^{\mathrm{proj}}(\sigma) = \mathbf{r}_0^{\mathrm{proj}} + \mathbf{r}_0^{\mathrm{proj}\,\prime}\tilde{\sigma} + \frac{1}{2}\mathbf{r}_0^{\mathrm{proj}\,\prime\prime}\tilde{\sigma}^2 + O(\tilde{\sigma}^2) \qquad \mathbf{r}_0^{\mathrm{proj}\,\prime} \cdot \mathbf{r}_0^{\mathrm{proj}\,\prime\prime} = 0 \tag{6.16}$$

where

$$\begin{aligned}
\mathbf{r}_0^{\mathrm{proj}}(\tilde{\tau}) \equiv\ & (\hat{\mathbf{m}} \cdot \hat{\mathbf{k}})\hat{\mathbf{k}}\,\tilde{\tau} \\
& - \left\{ \left[\frac{1}{2}\left(1 + \frac{(\vec{\mathbf{r}}_0 \cdot \dot{\mathbf{r}}'_0)^2}{|\vec{\mathbf{r}}_0|^4}\right)(\vec{\mathbf{r}}_0 \cdot \hat{\mathbf{k}}) - \left(\frac{\vec{\mathbf{r}}_0 \cdot \dot{\mathbf{r}}'_0}{|\vec{\mathbf{r}}_0|^2}\right)(\dot{\mathbf{r}}'_0 \cdot \hat{\mathbf{k}}) \right] \frac{\hat{\mathbf{m}} - \hat{\mathbf{k}}}{1 - \hat{\mathbf{m}} \cdot \hat{\mathbf{k}}}, \right. \\
& \left. + \frac{1}{2}\left[1 + \frac{(\vec{\mathbf{r}}_0 \cdot \dot{\mathbf{r}}'_0)^2}{|\vec{\mathbf{r}}_0|^4}\right]\vec{\mathbf{r}}_0 - \left[\frac{\vec{\mathbf{r}}_0 \cdot \dot{\mathbf{r}}'_0}{|\vec{\mathbf{r}}_0|^2}\right]\dot{\mathbf{r}}'_0 \right\}\tilde{\tau}^2 + O(\tilde{\tau}^3)
\end{aligned}$$

$$\mathbf{r}_0^{\mathrm{proj}\,\prime} = \left[\left((\dot{\mathbf{r}}'_0 \cdot \hat{\mathbf{k}}) - \frac{(\vec{\mathbf{r}}_0 \cdot \dot{\mathbf{r}}'_0)}{|\vec{\mathbf{r}}_0|^2}(\vec{\mathbf{r}}_0 \cdot \hat{\mathbf{k}}) \right) \frac{\hat{\mathbf{m}} - \hat{\mathbf{k}}}{1 - \hat{\mathbf{m}} \cdot \hat{\mathbf{k}}} + \dot{\mathbf{r}}'_0 - \frac{\vec{\mathbf{r}}_0 \cdot \dot{\mathbf{r}}'_0}{|\vec{\mathbf{r}}_0|^2}\vec{\mathbf{r}}_0 \right] \tilde{\tau} + O(\tilde{\tau}^2),$$

$$|\mathbf{r}_0^{\mathrm{proj}\,\prime}|^2 = \frac{|\vec{\mathbf{r}}_0|^2|\dot{\mathbf{r}}'_0|^2 - (\vec{\mathbf{r}}_0 \cdot \dot{\mathbf{r}}'_0)^2}{|\vec{\mathbf{r}}_0|^2}\tilde{\tau}^2 + O(\tilde{\tau}^3)$$

and

$$\mathbf{r}_0^{\mathrm{proj}\,\prime\prime} = \vec{\mathbf{r}}_0 + (\vec{\mathbf{r}}_0 \cdot \hat{\mathbf{k}})\frac{\hat{\mathbf{m}} - \hat{\mathbf{k}}}{1 - \hat{\mathbf{m}} \cdot \hat{\mathbf{k}}} + O(\tilde{\tau}) \qquad |\mathbf{r}_0^{\mathrm{proj}\,\prime\prime}| = |\vec{\mathbf{r}}_0| + O(\tilde{\tau}).$$

Thus the trajectory of the tip of the parabola for varying $\tilde{\tau}$ is also a parabola. One can show that

$$\mathbf{u} = \mathbf{u}_0 + O(\tilde{\sigma}) \qquad \mathbf{u}_0 = \hat{\mathbf{m}} - (\hat{\mathbf{m}} \cdot \hat{\mathbf{k}})\hat{\mathbf{k}} + O(\tilde{\tau}). \tag{6.17}$$

To parameterize the photon we use δ and θ defined by (see Figure 3)

$$\mathbf{x}_\perp - \mathbf{r}_0^{\mathrm{proj}} = \delta \left(\frac{\mathbf{r}_0^{\mathrm{proj}\,\prime\prime}}{|\mathbf{r}_0^{\mathrm{proj}\,\prime\prime}|} \cos\theta + \frac{\mathbf{r}_0^{\mathrm{proj}\,\prime}}{|\mathbf{r}_0^{\mathrm{proj}\,\prime}|} \sin\theta \right) \qquad \delta = |\mathbf{x}_\perp - \mathbf{r}_0^{\mathrm{proj}}| \tag{6.18}$$

We wish to calculate the photon boost in the limit of small δ and $\tilde{\tau}$. Expanding the integrand of (5.16) for small δ, τ, and $\tilde{\sigma}$ we find

$$\begin{aligned} \frac{\mathbf{u} \cdot (\mathbf{x}_\perp - \mathbf{r}^{\mathrm{proj}})}{|\mathbf{x}_\perp - \mathbf{r}^{\mathrm{proj}}|^2} =& \frac{\frac{\mathbf{u}_0 \cdot \mathbf{r}_0^{\mathrm{proj}\,\prime\prime}}{|\mathbf{r}_0^{\mathrm{proj}\,\prime\prime}|}(\delta\cos\theta - |\mathbf{r}_0^{\mathrm{proj}\,\prime\prime}|\tilde{\sigma}^2) + \frac{\mathbf{u}_0 \cdot \mathbf{r}_0^{\mathrm{proj}\,\prime}}{|\mathbf{r}_0^{\mathrm{proj}\,\prime}|}(\delta\sin\theta - |\mathbf{r}_0^{\mathrm{proj}\,\prime}|\tilde{\sigma})}{(\delta\cos\theta - |\mathbf{r}_0^{\mathrm{proj}\,\prime\prime}|\tilde{\sigma}^2)^2 + (\delta\sin\theta - |\mathbf{r}_0^{\mathrm{proj}\,\prime}|\tilde{\sigma})^2} + O(\sigma, \delta) \\ =& \frac{E\,(\delta\cos\theta - G\tilde{\sigma}^2) + F\,(\delta\sin\theta - H\tilde{\tau}\tilde{\sigma})}{(\delta\cos\theta - G\tilde{\sigma}^2)^2 + (\delta\sin\theta - H\tilde{\tau}\tilde{\sigma})^2} + O(\tilde{\sigma}, \tilde{\tau}, \delta) \end{aligned} \tag{6.19}$$

where

$$E = \frac{\dot{\mathbf{r}}_0 \cdot \hat{\mathbf{k}}}{|\dot{\mathbf{r}}_0|}, \qquad G = |\dot{\mathbf{r}}_0|, \qquad H = \frac{\sqrt{|\dot{\mathbf{r}}_0|^2 |\dot{\mathbf{r}}_0'|^2 - (\dot{\mathbf{r}}_0 \cdot \dot{\mathbf{r}}_0')^2}}{|\dot{\mathbf{r}}_0|},$$

and

$$F = \frac{|\dot{\mathbf{r}}_0|^2 (\dot{\mathbf{r}}_0' \cdot \hat{\mathbf{k}}) - (\dot{\mathbf{r}}_0 \cdot \dot{\mathbf{r}}_0')(\dot{\mathbf{r}}_0 \cdot \hat{\mathbf{k}})}{|\dot{\mathbf{r}}_0| \sqrt{|\dot{\mathbf{r}}_0|^2 |\dot{\mathbf{r}}_0'|^2 - (\dot{\mathbf{r}}_0 \cdot \dot{\mathbf{r}}_0')^2}}.$$

For $\tilde{\sigma} = \tilde{\tau} = \delta = 0$ the integrand diverges and for the δ and $\tilde{\tau}$ small, there is a region near $\tilde{\sigma} = 0$ where the integrand is large. Away from this region the integrand falls off as $\tilde{\sigma}^{-4}$ until $\tilde{\sigma}$ is so large that the approximations used to derive (6.19) is invalid. Approximating the full integral (5.16) by the integral of (6.19) over the interval $\tilde{\sigma} \in (-\infty, +\infty)$ is a good approximation as long as

$$\delta,\, \tilde{\tau} \ll |\dot{\mathbf{r}}_0|^{-1},\, |\dot{\mathbf{r}}_0'|^{-1}. \tag{6.20}$$

Thus as long as (6.20) is satisfied the anisotropy pattern near a cusp is approximately

$$\frac{\Delta T}{T} \cong -4\tilde{\mu} \int_{-\infty}^{+\infty} \frac{E\,(\delta\cos\theta - G\tilde{\sigma}^2) + F\,(\delta\sin\theta - H\tilde{\tau}\tilde{\sigma})}{(\delta\cos\theta - G\tilde{\sigma}^2)^2 + (\delta\sin\theta - H\tilde{\tau}\tilde{\sigma})^2} d\tilde{\sigma} \tag{6.21}$$

Unfortunately, as far as the author knows, this function cannot be integrated in terms of simple functions. One may integrate (6.21) in terms of simple functions if one may ignore the term $H\tilde{\sigma}\tilde{\tau}$. This approximation is equivalent to taking $\mathbf{r}_0^{\mathrm{proj}\,\prime} = 0$. The curve traced by the string on the sky is thus approximated as a half-line and not a parabola. The approximation is good if $\dot{\mathbf{r}}_0'$ is nearly parallel or anti-parallel to $\dot{\mathbf{r}}_0$ or if $|\tilde{\tau}| \ll \delta$. Thus this is appropriate for any geometry very near the time one sees the actual cusp. Unfortunately this solution does not tell us much about the temporal behavior of the anisotropy pattern, the result being independent of $\tilde{\tau}$. In this limit

$$F \to \pm \frac{\sqrt{(1 - \mathbf{m} \cdot \hat{\mathbf{k}})^2 |\dot{\mathbf{r}}_0|^2 - (\dot{\mathbf{r}}_0 \cdot \hat{\mathbf{k}})^2}}{|\dot{\mathbf{r}}_0|}. \tag{6.22}$$

The sign depends on how $\dot{\vec{r}}_0'$ approaches either $\vec{r}_0$ or $-\vec{r}_0$. The temperature pattern then approaches

$$\frac{\Delta T}{T} = \frac{4\pi}{\sqrt{2}}\tilde{\mu}\frac{1}{\sqrt{|\vec{r}_0|^3\delta}}\left(\frac{1}{2}\vec{r}_0\cdot\hat{\mathbf{k}}\sqrt{1-\cos\theta} \pm \sqrt{(1-\mathbf{m}\cdot\hat{\mathbf{k}})^2|\vec{r}_0|^2 - (\vec{r}_0\cdot\hat{\mathbf{k}})^2}\frac{\sin\theta}{\sqrt{1-\cos\theta}}\right). \tag{6.23}$$

The temperature pattern diverges as $\delta^{-1/2}$ as one approaches the tip of the cusp from any direction. The angular dependence around the cusp consists of two terms. Both are zero on the line segment $\theta = \pi/2$. The first term takes only one sign, going from zero to its extremal value as θ goes from π to 0 or from π to 2π. The second term is odd in θ and discontinuous at $\theta = 0$, i.e. across the string. The magnitude of the discontinuity diverges as one approaches the tip of the cusp, just as expected.

If the angular scale corresponding to $|\vec{r}_0|^{-1}$ is much greater than the resolution of a detector then the detector response near a cusp could be much greater than the signal near other parts of the string. The effect is a much stronger than for the kink as the $\delta^{-1/2}$ growth is faster than $\ln\delta$. Even thought the maximal temperature deviation diverges in (6.23), the area integrated temperature remains finite. This is not due to cancellation, but rather is due to the increasingly small angular areas covered by the increasingly large temperature deviations. We see that cusps give only finite contributions to the r.m.s. temperature deviation. The condition $|\tilde{r}| \ll \delta$ for the validity of (6.23) and the form of (6.23) is evidence that the maximal anisotropy goes as $|\tilde{r}|^{-1/2}$ in the general case, $\tilde{r} \neq 0$.

Warning

In the preceding subsections the anisotropy pattern very close to a piece of string was considered. It is expected that the component of the MBR anisotropy that will dominate in this case is the one that is being studied in this paper, i.e. that from the the sub-horizon peculiar gravitational fields of the string. On larger scales both corrections due to the expanding universe and from other sources of anisotropy will contribute. In what follows we discuss aspects of the anisotropy without the restriction that one is looking very close to the string. Thus it should be understood that we are only discussing the component of anisotropy from the peculiar gravitational field of the loop, and that referring to the anisotropy pattern within a horizon size of a loop. The smallest horizon size of interest is that at the redshift of last scattering. If there were no significant reheating then this would take place at a $z \sim 1000$ and the associated angular scale would be $\sim 0.5°$. If reheating did occur then the surface of last-scattering could only be moved to a lower redshift and the corresponding angular scale be larger. Thus corrections due to expansion should only be important for angular scales comparable to or larger than 0.5°.

Anisotropy Far From a Loop

We now consider the pattern of anisotropy very far from the loop. Far meaning those photons which have impact parameters much greater than the loop size, but not so far as to invalidate the small angle approximation. We choose the coordinates so that at $t' = 0$ the loop center-of-mass lies near the coordinate origin. As the temperature pattern away from the loop obeys Laplace's equation in two dimensions (see below) we may use the standard expansion of solutions of the two-dimensional Laplace equation in circular coordinates. This

infinite expansion converges to the correct pattern for $|\mathbf{x}_\perp| > \max_\sigma |\mathbf{r}(\sigma, t'^p_{\max}(\sigma)|$. The nth term in the expansion falls off as $|\mathbf{x}_\perp|^{-n}$ and has sinusoidal angular dependence with period $2\pi/n$. The first two terms have period 2π and π and will be referred to as the asymptotic dipole pattern and the asymptotic quadrupole pattern, respectively. The dipole term, if non-zero, will dominate for sufficiently large impact parameters. For the loops that we study in §VII we have found that there exists ranges of impact parameters, $|\mathbf{x}_\perp|$, for which the quadrupole term dominates. This has not been found to be true for the higher order terms. We only explicitly write the dipole and quadrupole terms:

$$\frac{\Delta T}{T} = -4\tilde{\mu}\left(\frac{\mathbf{x}_\perp \cdot \mathbf{d}}{|\mathbf{x}_\perp|^2} + \frac{x^i_\perp x^j_\perp Q_{ij}}{|\mathbf{x}_\perp|^4} + ...\right) \tag{6.24}$$

where

$$\mathbf{d} \equiv \oint \mathbf{u}\, d\sigma \qquad \text{and} \qquad Q_{ij} \equiv \oint (u^i r^{\rm proj}_j + r^{\rm proj}_i u^j - \mathbf{u}\cdot\mathbf{r}^{\rm proj}\delta^i_j)\, d\sigma.$$

For a loop with no net momentum, dimensional analysis suggests that the magnitude of the dipole and quadrupole integrals should be $\sim L$ and $\sim L^2$, respectively, where L is the length of the loop. For the specific cases studied below it was found that this is a large overestimate for the dipole term but a reasonable estimate for the quadrupole term.

The asymptotic dipole temperature pattern very far from the loop has the same form as the temperature pattern around a moving point mass (see §IV). Note that while for a point mass the magnitude and direction of $\mathbf{d}$ is given by the momentum of the point mass, this is not true for a loop. The direction and magnitude of the dipole pattern will, in general, oscillate as the loop oscillates. (One exception which is unlikely to occur in practice is a loop configuration that moves entirely in a plane perpendicular to the line of sight. In this case the dipole pattern is the same as for a point mass with the same momentum as the loop and the dipole vector is therefore constant in direction and magnitude.) The difference between the point mass and the loop is that a loop has relativistic internal motion. The magnitude of the oscillatory part of $\mathbf{d}$ is an observable measure of how relativistic the internal motions of an object is.

Unresolved Loops

It will also be important to consider the contribution of loops much smaller than the detector beam-size to the signal obtained by a detector. The relevant pattern is the temperature pattern convolved with the beam. One might think that for a sufficiently large beam with a loop near its center this is equivalent to the integral of the temperature pattern of the loop over the entire sky. This turns out not to be quite true. The value of detector response depends on exactly where the loop is placed with respect to the beam, even if the loop is in a region where the detector response is flat. Consider a detector with a circularly symmetric beam pattern $B(\theta)$. If the angular size of the loop and the angular size of the beam are both small then the detector response will be approximately proportional to the integral of the brightness pattern over a disc in the $\mathbf{x}_\perp$ plane. Let us put circular coordinates on the $\mathbf{x}_\perp$ plane with $r = 0$ at the beam center and let d_l be the distance to the loop or, in a cosmological setting, the angular diameter distance (see Weinberg 1972 Chapter 14 §4). The

contribution the anisotropy pattern of a loop to the detector response is then

$$\delta\mathcal{R} \equiv \int \frac{\Delta T}{T} B(\frac{r}{d_l}) \frac{d^2\mathbf{x}_\perp}{d_l^2} = -\frac{4\tilde{\mu}}{d_l^2} \oint \int_0^\infty B(\frac{r}{d_l}) \int_0^{2\pi} \frac{\mathbf{u}\cdot(\mathbf{x}_\perp - \mathbf{r}^{\rm proj})}{|\mathbf{x}_\perp - \mathbf{r}^{\rm proj}|^2} d\phi\, r\, dr\, d\sigma$$
$$= \frac{4\pi\tilde{\mu}}{d_l^2} \oint B(\frac{|\mathbf{r}^{\rm proj}|}{d_l}) \mathbf{u}\cdot\mathbf{r}^{\rm proj}\, d\sigma \tag{6.25}$$

First note that the response is independent of the beam pattern except at parts of the beam that include the loop (This would not be true if the beam were not circularly symmetric). Second notice that the response depends on the position of the beam center even if the detector has flat response over the entire locus of the loop and to angles much larger than the angular size of the loop. In general one expects unresolved sources to give a constant signal independent of the beam center as long as they remain in the a part of the beam where the sensitivity is constant. The reason that this is not true for loops is that the asymptotic dipole pattern falls off sufficiently slowly with impact parameter that the "sidelobes" of this pattern can dominate the signal from unresolved loops.

Now let us consider loops that are much smaller than the beam. Let $\mathbf{r}_0$ be the distance in the $\mathbf{x}_\perp$ plane of the loop from the beam center. If the loop is very small then $\mathbf{r}^{\rm proj}$ will not deviate much from $\mathbf{r}_0$ and (6.25) becomes

$$\delta\mathcal{R} = 4\pi\tilde{\mu} B(\frac{|\mathbf{r}_0|}{d_l}) \frac{\mathbf{d}\cdot\mathbf{r}_0}{d_l^2} \tag{6.26}$$

where $\mathbf{d}$ is the dipole vector defined in the previous subsection. A given loop will give the maximal signal not at the beam center but where $|\mathbf{r}_0| B(|\mathbf{r}_0|/d_l)$ is maximized which is generally about one beam-radius away from center. Furthermore note that the signal from a very small loop scales with its mass ($\propto L \propto |\mathbf{d}|$) and not with its mass squared (which gives the projected area of the loop). The sign of the signal depends on the relative orientation of $\mathbf{d}$ and $\mathbf{r}_0$. If one had a random distribution of unresolved loops one would therefore expect that the expected rms signal from this population would scale as square root of their angular number density.

Laplace's Equation

Given the expression, (5.16), for the temperature pattern on the sky one can easily show that

$$\nabla^2 \frac{\Delta T}{T} = -8\pi\,\tilde{\mu} \oint \mathbf{u}\cdot\nabla_{\mathbf{x}_\perp} \delta^{(2)}(\mathbf{x}_\perp - \mathbf{r}^{\rm proj})\, d\sigma. \tag{6.27}$$

Thus the temperature pattern, except at points passing through a piece of string, will obey the two-dimensional Laplace's equation. This has several important consequences.

Several identities are known for solutions to Laplace's equations which may be exploited to compute quantitative estimates of some aspects of the anisotropy expected from strings easily. We shall leave this to the second paper and concentrate on the qualitative consequences of (6.27). It is well known that solutions to Laplace's equations have no local maxima or minima except at boundaries. We thus know that there will be no local temperature maxima or minima except where the string is. It is also well known that the solutions to

Laplace's equation are fully determined by their boundary conditions. Thus we learn no additional information about the loop configuration by measuring the anisotropy pattern away from where we see the temperature jumps. If strings were discovered and we had low-noise, high-resolution maps of the MBR temperature, then one could check whether the Laplace equation was satisfied as a test of the theory. However, contamination by other sources of anisotropy might make this difficult. Schemes may be discovered, using equation (6.27) and the fact that only this component of the anisotropy produces temperature jumps, to subtract off other components from the overall temperature pattern. However, since the boundary condition for the Laplace equation must involve more than the temperature jump, this is not straightforward.

Finally we bring to the attention of the reader a helpful analogy that can be made between the formalism that we have developed here and two-dimensional electrostatics. First note that equation (6.27) combined with the boundary conditions that $\Delta T/T$ fall to zero far from the loop is not merely a consequence of equation (5.16) but is completely equivalent to the original formulation. Equation (6.27) is of the form of Poisson's equation in two dimensions. The source term being the sum of gradients of δ-functions is equivalent to a sum of idealized infinitesimal dipoles, i.e. two equal and opposite charges an infinitesimal distance apart such that the product of the charge times the separation is finite. The magnitude and direction of the dipole moment is given by the vector $\mathbf{u}$ which depends among other things on the velocity of the string at that point. The sum is, of course, the σ integral and the dipoles thus lie along the curve traced out by the string on the sky. The temperature pattern is the same as the electrostatic potential produced by such a configuration of charges. With this analogy we can easily understand the logarithmic term in anisotropy around a kink. Equation (6.11) tells us that the temperature pattern around a kink has a component which depends logarithmically on the magnitude of the impact parameter from the kink. The prefactor of the logarithm depends on the component of $\mathbf{u}_1$ and $\mathbf{u}_2$ parallel to length of string segment 1 and 2, respectively. For a straight string of dipoles with uniform dipole density and direction parallel to the string there is complete cancellation of charge except at the endpoints. At the endpoint there is an isolated charge, which in two dimensions has a potential which depends logarithmically on the distance from the endpoint. Thus the prefactor of the logarithm in equation (6.11) is analogous to the sum of the endpoint charge on the two segments which meet at the kink.

VII. THE SIMPLEST LOOP

It is apparent that equation (3.30) simplifies greatly if the loop configuration remains in a plane which is perpendicular to the direction of photon propagation, $\hat{\mathbf{k}}$. In this case $\dot{\mathbf{r}}\cdot\hat{\mathbf{k}}$, $\bar{\mathbf{r}}\cdot\hat{\mathbf{k}}$, and $\mathbf{r}'\cdot\hat{\mathbf{k}}$ are all zero and $S(\sigma,t)=\frac{1}{2}\tilde{\mu}$. Furthermore, one may choose $\mathbf{x}_0$ and the spacetime coordinate system such that $\mathbf{r}\cdot\hat{\mathbf{k}}$ is zero (i.e. $\bar{\mathbf{r}}\cdot\hat{\mathbf{k}}=0$), so that $t'^{p}_{\max}=\tau$ for all parts of the string. With these simplifying assumptions equation (5.16) becomes

$$\frac{\Delta E}{E}=-4\tilde{\mu}\oint\left[\frac{\dot{\mathbf{r}}\cdot(\mathbf{x}_\perp-\mathbf{r})}{|\mathbf{x}_\perp-\mathbf{r}|^2}\right]_{t'=\tau}d\sigma=-4\tilde{\mu}\left[\frac{\partial}{\partial\tau}\left(\oint\ln|\mathbf{x}_\perp-\mathbf{r}|\,d\sigma\right)\right]_{t'=\tau}. \qquad (7.1)$$

The relevance of this case is to planar loops seen face-on from a distance much greater than the size of the loop, as discussed at the end of §III. If the planar loop is not moving then $\mathbf{r}$ will

be periodic. The later form of equation (7.1) then tells us that at any given position in the sky, $\mathbf{x}_\perp$, the time averaged temperature deviation is zero. This follows from the fact that the time of observation is just linearly related to τ. We would expect the loops that we observe to be at random phases in their oscillations. It then follows that the expected temperature deviation at any point (i.e. irrespective of the position of the loop) is zero. Of course, this analysis only applies to flat face-on stationary loops. It is not true that at any given time that the angle-averaged anisotropy is zero, as shall now be shown using a specific example.

The simplest possible loop configuration is a circular loops whose radius just oscillates. Such a solution is given by equation (5.13) with $\alpha = 1$ and $\phi = 0$. Taking $\psi = 0$, the loop configuration is given by

$$\mathbf{r}(\sigma, t') = \frac{L}{2\pi}\cos(\frac{2\pi t'}{L})\left(\cos(\frac{2\pi\sigma}{L})\,\hat{\mathbf{x}} + \sin(\frac{2\pi\sigma}{L})\,\hat{\mathbf{y}}\right) \tag{7.2}$$

where we have taken the origin of coordinates to be the center of the circle. The radius of the circle just oscillates sinusoidally, and τ gives the time at which the observer sees the loop. Such a configuration is somewhat unusual since the loop goes to a point once each period. This type of singular behavior does not occur except for very symmetric loops and is therefore not generic. If general relativistic effects were included, then such a loops would form a black hole and not reexpand. Furthermore, the linear approximation to the gravitational fields used in this paper would not be valid near the point singularity. Thus we would expect some singular behavior in the boost of a photon passing near this singularity in space and time. The behavior of photons passing near a singular point is not of general interest since it is unlikely to occur in practice.

For the trajectory of equation (7.1) we must take $\hat{\mathbf{k}} = \pm\hat{\mathbf{z}}$ for equation (7.1) to be valid. We will chose $\hat{\mathbf{k}} = \hat{\mathbf{z}}$, so the observer's z coordinate has a large (compared with L) positive value. We will parameterize $\mathbf{x}_0$ by

$$\mathbf{x}_0 = R_\gamma\,(\cos\phi\;\hat{\mathbf{x}} + \sin\phi\;\hat{\mathbf{y}} - \tau\;\hat{\mathbf{z}}) \tag{7.3}$$

The geometry is circularly symmetric, so the boost of the photon should only depend R_γ and not on ϕ. One may perform the integral (7.1) analytically, obtaining

$$\frac{\Delta E}{E} = \frac{\Delta T}{T} = \begin{cases} 8\pi\tilde{\mu}\,\tan\left(\frac{2\pi\tau}{L}\right) & R_\gamma < \left|\cos\left(\frac{2\pi\tau}{L}\right)\right| \\ 0 & R_\gamma > \left|\cos\left(\frac{2\pi\tau}{L}\right)\right| \end{cases}. \tag{7.4}$$

Thus the temperature pattern on the sky of the observer will be a circular "top hat", and there will be no temperature deviations outside of the projection of the loop. Note that the temperature pattern only depends on $\tau \bmod L/2$ and not $\tau \bmod L$. This is because, as mentioned in §V, the actual period of the loop is half the period of the individual particles. It is easily verified that the temperature discontinuity equation (6.1) is satisfied. The temperature deviation inside the top hat diverges as the loop goes to a point. However, we see that the signal received by a fixed beam-size detector would actually go to zero, because while the temperature deviation is increasing the angular size of the top hat is decreasing faster. Of course, a circular loop seen face-on, or any other flat face-on loop is a very special case. One

should not expect any general properties of equation (7.1) to hold for all loops. This author knows of no loop configuration other than flat face-on loops for which equation (5.16) may be integrated in terms of simple functions. Thus the remainder of this paper is devoted to numerical results.

VIII. ANISOTROPY AROUND A SINGLE LOOP

In this section are presented the results of numerical integrations of the anisotropy around a single loop. The results presented here were obtained by integrating a spline fit to the integrand. This spline fit was obtained by evaluations of the function on a grid of points. The point spacing of the spline grid was variable, and the grid was chosen to give finer spacing where the function was rapidly varying. In preliminary computations other integration methods were used in which an error estimate was obtainable. It was found that the spline method is generally good to within 1%. This is, however, not always the case. Some problem occurs when the photon in consideration came very close to part of the loop, in which case some parts of the integrand are extremely rapidly varying functions (see §VI). The spline method was chosen because it was less prone to catastrophic failure in these cases, although the accuracy at these points is not particularly good. There are, however, photon trajectories for which the spline method, as implemented failed. These will be referred to as "bad points".

Photon trajectories were laid out on a 150×150 grid centered on the center of mass of this loop. The length of each side of the grid is $3\pi/4$ times the length of the loop as it is defined in equatiion (5.4). The fractional temperature boost was calculated for each grid point to form an image of the temperature pattern near the loop on the sky. Each image required $\sim$ 3.5 cpu hours on a VAX 11/780 to compute the integrals. The images are presented as halftones. The quality of the halftone plotter used is not particularly good, there being significant variations in the boldness with which dots are printed on a given page. To compensate for this, each image is displayed 3 times as a halftone plot, each with different choices of saturation temperature. The three saturation points being the same for all images. Here saturation means all black or all white. The values chosen are $\pm 5\tilde{\mu}$, $\pm 15\tilde{\mu}$, and $\pm 45\tilde{\mu}$. This allows the reader both sufficient dynamic range to gauge the anisotropy for all the images, and enough uniformity of presentation so the reader may compare different images. For the loop configurations presented in this section about five "bad points" were found in a typical image. Usually a bad point was found not to be next to another bad point. In the figures some of these bad points are identifiable as points which are saturated either positive or negative while the neighboring points are not.

The images computed are presented in Figure 4. For this figure we have restricted ourself to one particular loop configuration seen from a particular angle and viewed at nine different times during its oscillation. Note the anticorrelation between the size of the loop and the magnitude of the anisotropy near the loop. This is expected because when the loop is small, its parts are moving fast in order for the loop to reexpand. When the loop is near its maximum size it is moving slowly so the tension of the loop will cause it to recollapse before it gets much larger. In these plots the regions that are saturated are very pronounced. First consider the regions that are saturated with temperatures deviating more the $45\tilde{\mu}$ from the mean. There are very few such regions, the area of these regions being much less than the

FIGURE 4: Temperature pattern around certain loop configurations. The three grayscale images on the left of each figure represent the same temperature pattern but with a different relation between temperature and dot density. These relations are indicated in the scale in the upper right corner. Outside the limits of the scale the density of dots is saturated with either no dots or all the pixels being dotted. The quantity μ in the labels corresponds to the dimensionless quantity $\tilde{\mu}$ in the text. Also on the left is plotted the projection of the loop causing the anisotropy. Thin lines sticking out from the loop have a length proportional to $\beta_\perp \gamma$ which gives the magnitude of the discontinuity in temperature across the string. The label at the top of this plot gives the normalization. The temperature was computed on a square array of points filling the box. Below the loop projection is plotted a histogram of the base 10 logarithm of the number of points in certain temperature bins. Lowest horizontal tick mark corresponds to one point. Average temperature deviation is given below this, as is the rms deviation from zero. Loop configurationa are those of eq. (5.9), the two parameters α and ϕ indicated in the figures. Orientation of the loop is given by the angles θ_1 and θ_2 as follows: take the loop trajectory exactly as in eq. (5.9) with the observer at asymptotic infinity along the positive z axis; rotate the loop an angle θ_1 in the x-y plane from x to y about the origin; and then rotate the loop an angle θ_2 in the y-z plane from y to z. The third Euler angle just rotates the loop in the plane of the sky and is unimportant. The patch of sky plotted corresponds to photon trajectories in the $+z$ direction with x and y coordinates less than 1.5. The phase of the loop is given by ψ and is chosen so that the photons pass through the $z = 0$ plane at $t = \psi$.

mean projected area of the loop. There are larger regions saturated above $15\tilde{\mu}$ and, of course, still larger regions saturated above $5\tilde{\mu}$. The area of the latter regions being comparable to the mean projected size of the loop. Also presented in in Figure 4 is a histogram giving the distribution of temperatures. In most cases the tails of the distribution looks roughly exponential. While this falls off slower than a Gaussian, it is still fairly steep. Note, however, the large difference in the histograms of different images. It is dangerous to draw general conclusions from this one set of simulations, but, it seems reasonable to say that the anisotropy near a loop is typically $5 - 10\,\tilde{\mu}$. However, placing a constraint on possible values of $\tilde{\mu}$ from these few simulations and observations of MBR isotropy would be going too far. In any case, to obtain such constraints would require knowledge of the distribution of loop shapes and size on the sky. To determine, this one requires the knowledge of the distribution of loop size in the matter era. While the shape of the distribution and order of magnitude estimates of the normalization are easily obtainable, a detailed result is not. While this is an area of current research, no results are yet available.

IX. COMPARISON WITH PREVIOUS WORK

The aspect of MBR anisotropy examined in this paper has also been examined previously in the paper by Brandenberger, Albrecht, and Turok (1986). While they restricted their analysis to gravity waves, the present work includes all components of the gravitational field. They made some attempt to account for cosmological expansion while the present paper includes no such effects. Their approach was rather heuristic, they merely used an estimate for the amplitude and frequency of gravity waves at a given distance from a loop. In this sense their work was much less precise than that given here. If one were to apply their formalism to the case of photons passing by a loop with impact parameters much larger the loop size but much smaller than the horizon size at the time they passed the loop, one would conclude that the temperature perturbations given to the photons have no systematic dependence on the impact parameter. In their analysis the temperature pattern only falls off with increasing impact parameter due to cosmological effects which become important when the impact parameter is comparable to the horizon size. This contradicts the results derived in the present paper in which the temperature perturbation falls off at least as fast as the inverse of the impact parameter without including cosmological effects. The source of the

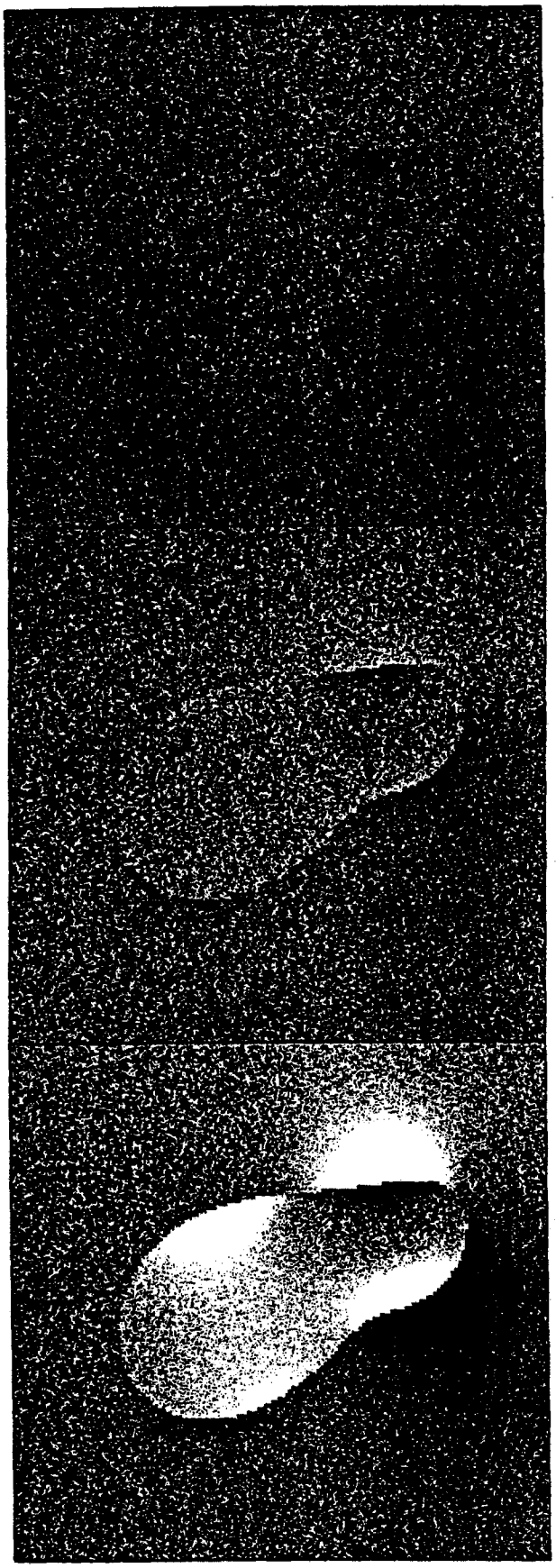

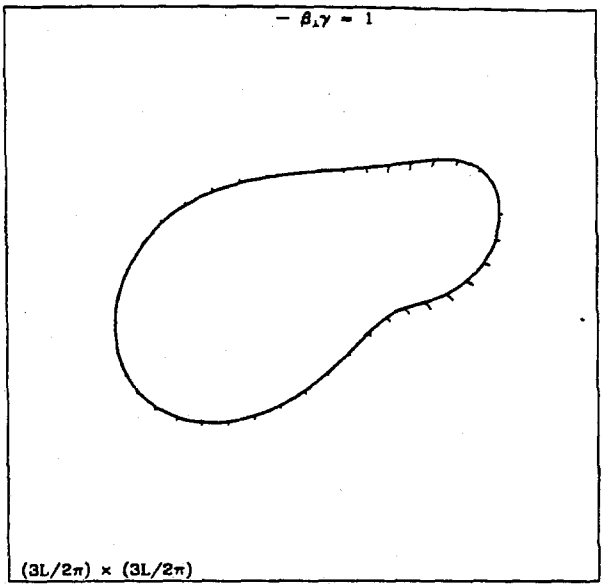

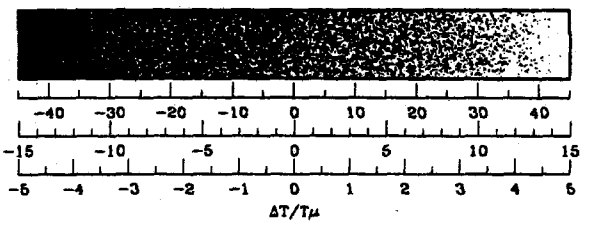

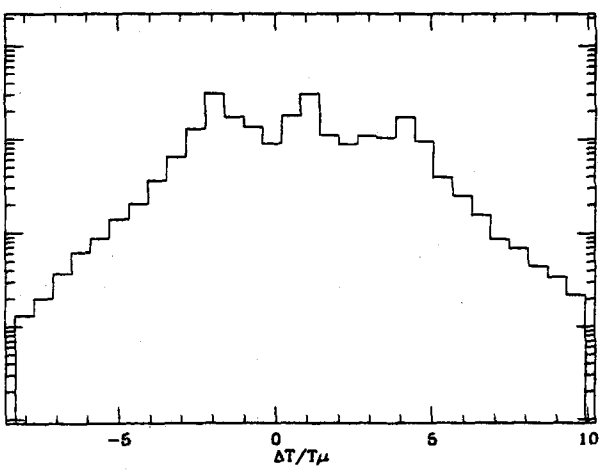

$\langle \Delta T/T \rangle = 0.64\ \mu$

$\langle \Delta T/T \rangle_{rms} = 2.82\ \mu$

$\alpha = 0.50000$

$\sin(\phi) = 0.50000$

$\psi = 0.000$

$\theta_1 = 50.000$

$\theta_2 = 50.000$

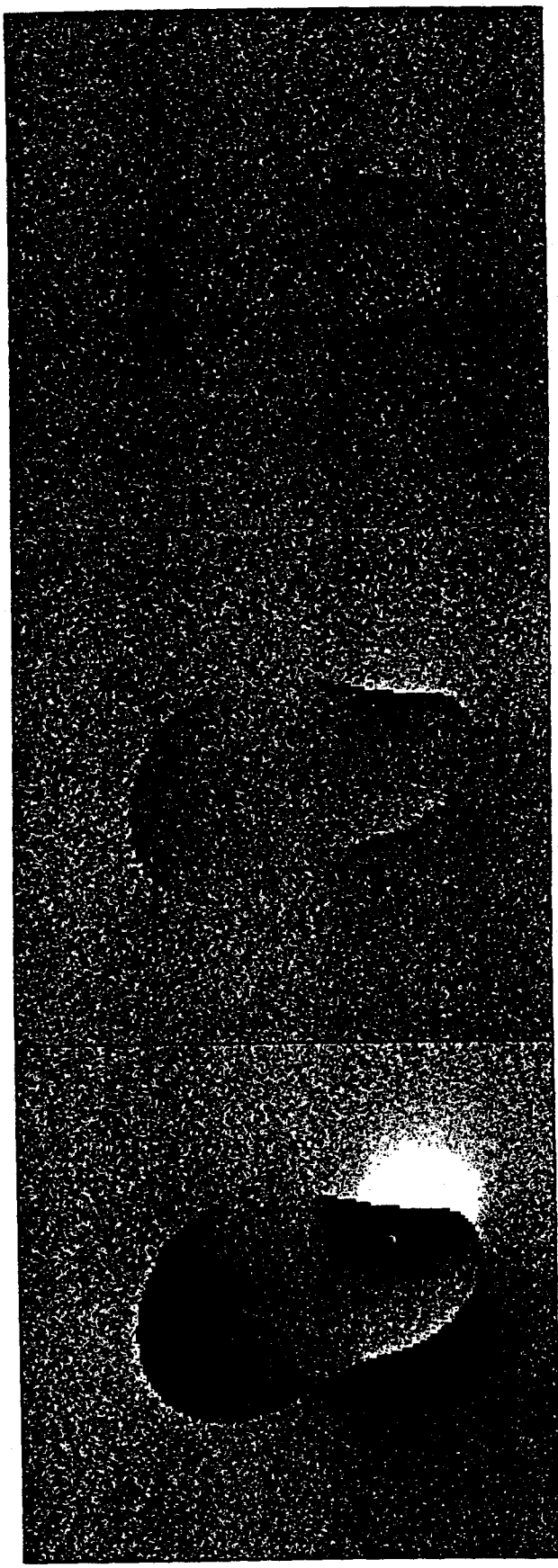

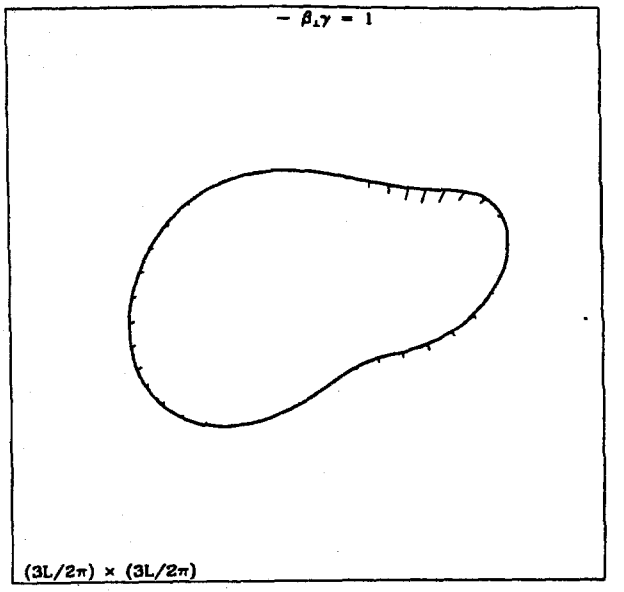

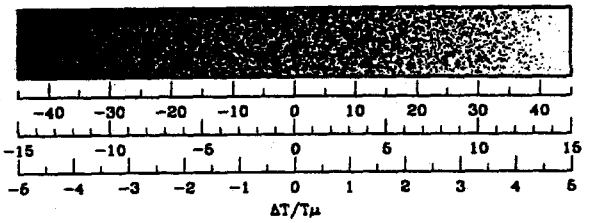

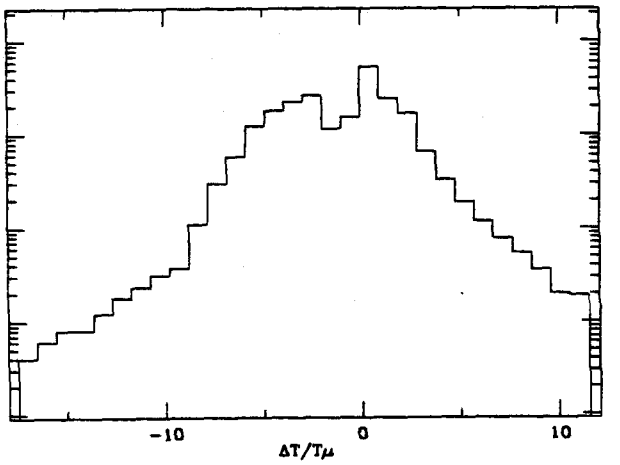

$\langle \Delta T/T \rangle = -1.01\ \mu$

$\langle \Delta T/T \rangle_{rms} = 3.22\ \mu$

$\alpha = 0.50000$

$\sin(\phi) = 0.50000$

$\psi = 20.000$

$\theta_1 = 50.000$

$\theta_2 = 50.000$

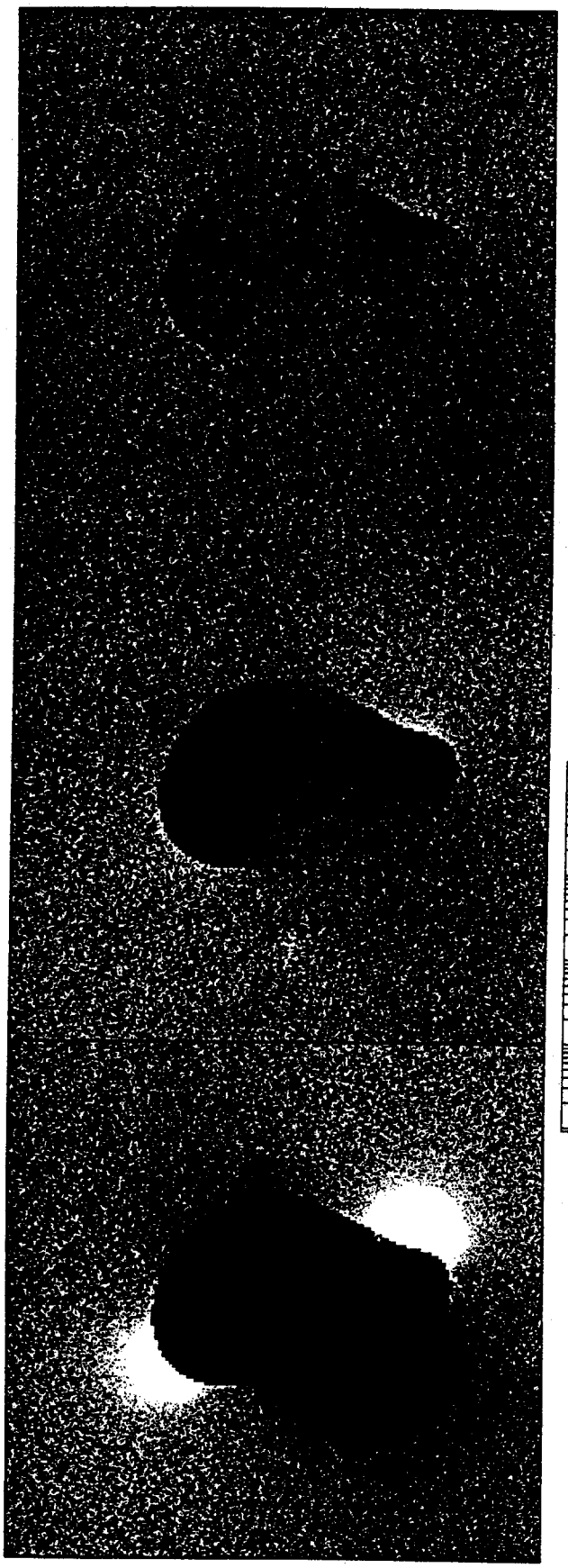

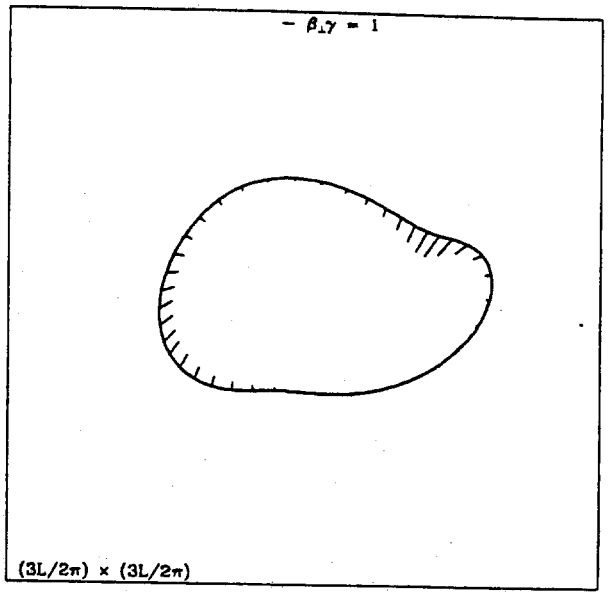

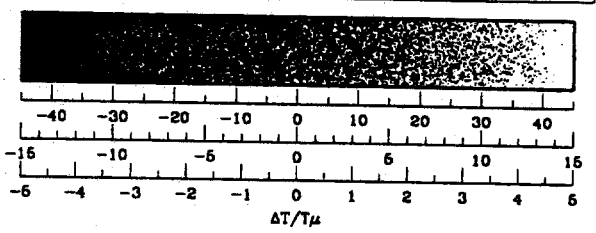

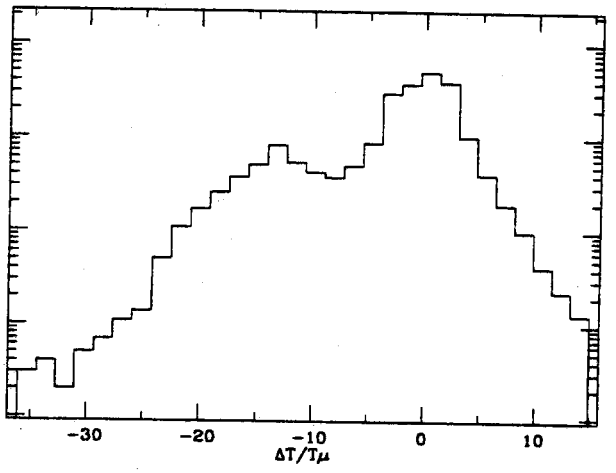

$\langle \Delta T/T \rangle = -2.32\ \mu$

$\langle \Delta T/T \rangle_{rms} = 6.34\ \mu$

$\alpha = 0.50000$

$\sin(\phi) = 0.50000$

$\psi = 40.000$

$\theta_1 = 50.000$

$\theta_2 = 50.000$

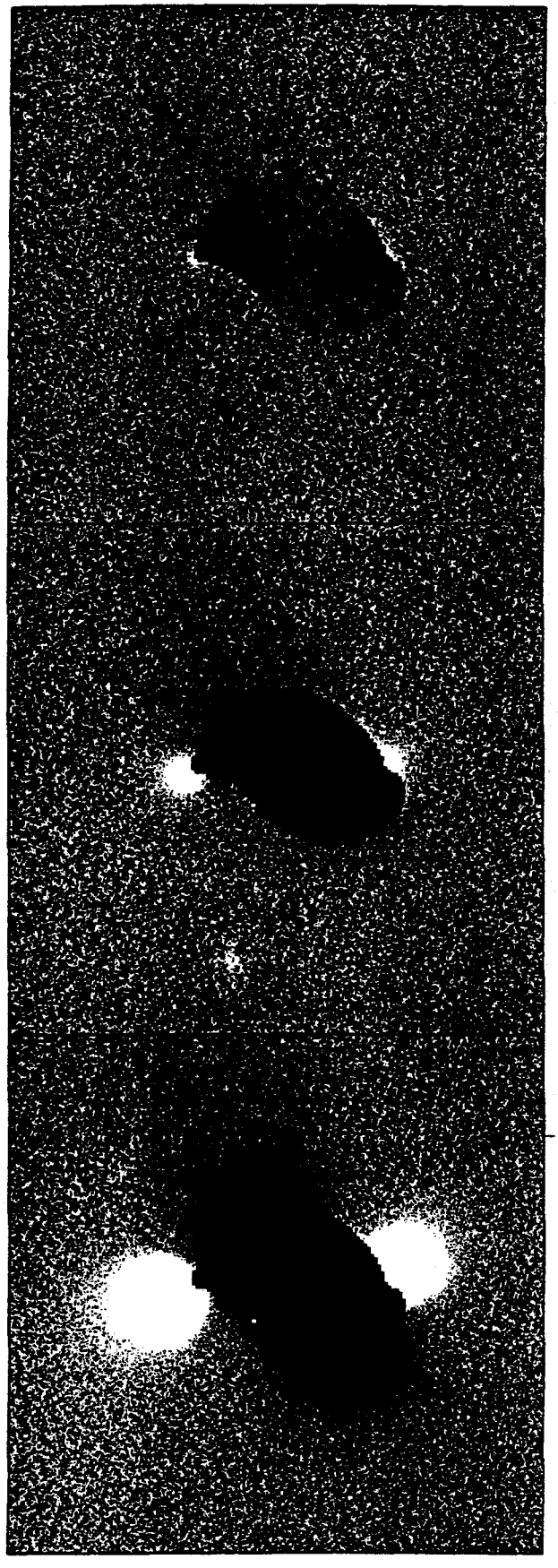

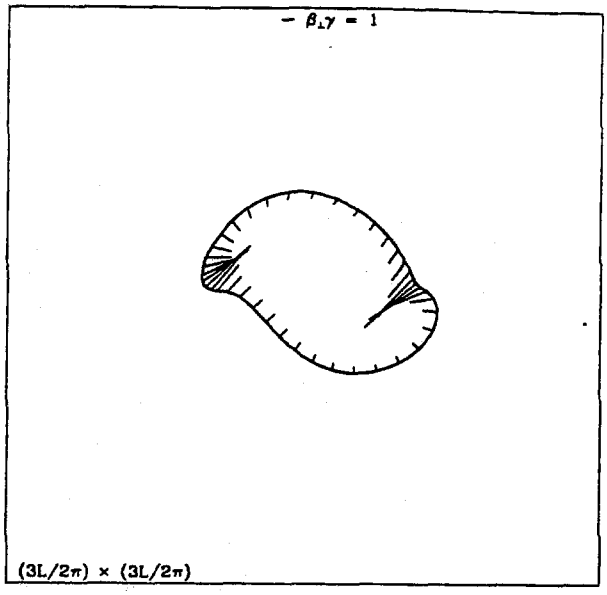

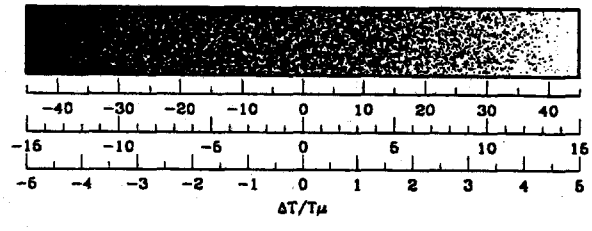

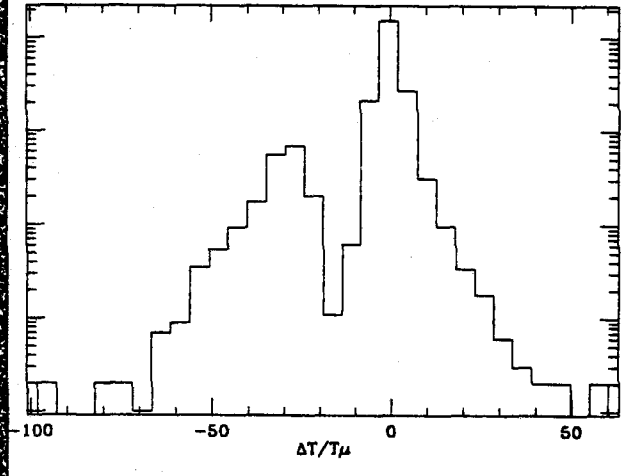

$\langle \Delta T/T \rangle = -2.58\ \mu$

$\langle \Delta T/T \rangle_{rms} = 9.73\ \mu$

$\alpha = 0.50000$

$\sin(\phi) = 0.50000$

$\psi = 60.000$

$\theta_1 = 50.000$

$\theta_2 = 50.000$

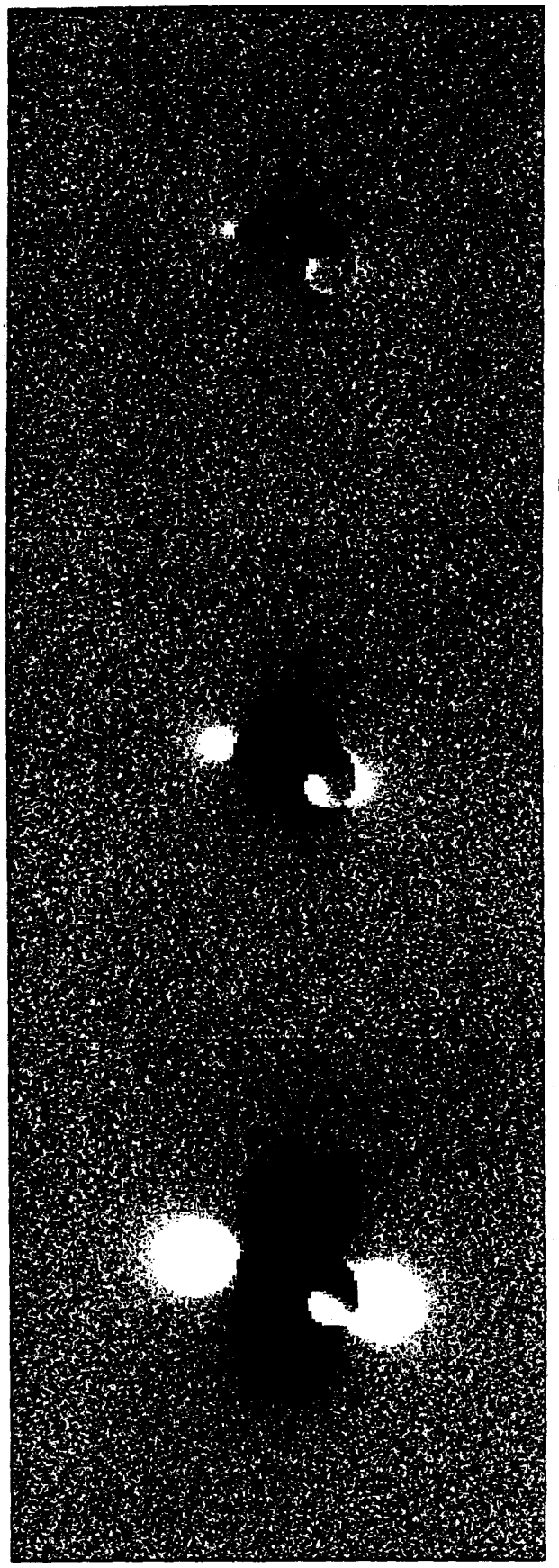

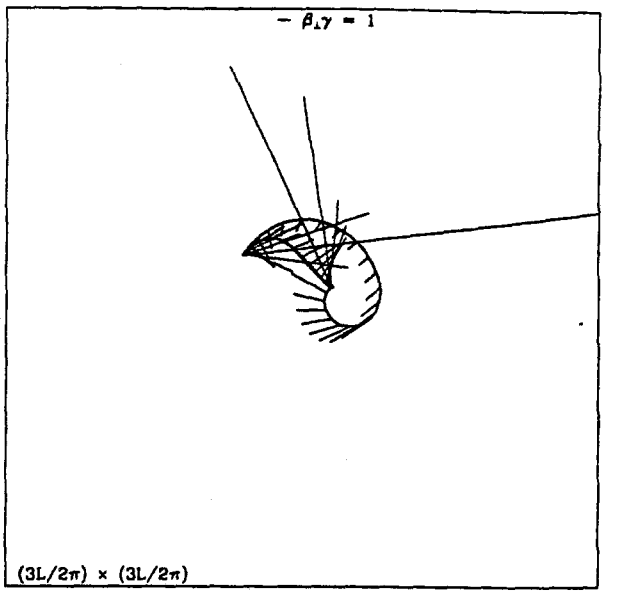

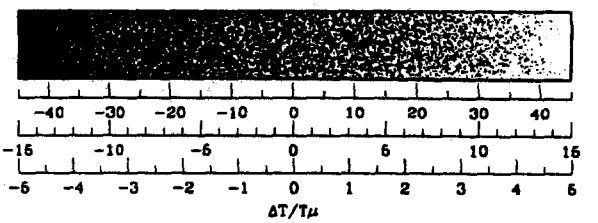

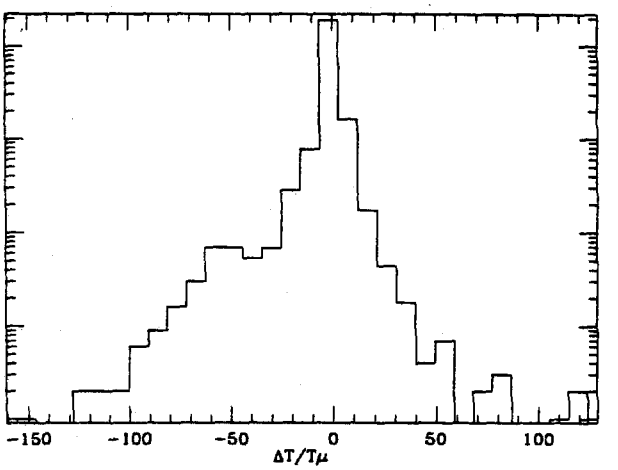

$\langle \Delta T/T \rangle = -1.04\ \mu$

$\langle \Delta T/T \rangle_{rms} = 8.06\ \mu$

$\alpha = 0.50000$

$\sin(\phi) = 0.50000$

$\psi = 80.000$

$\theta_1 = 50.000$

$\theta_2 = 50.000$

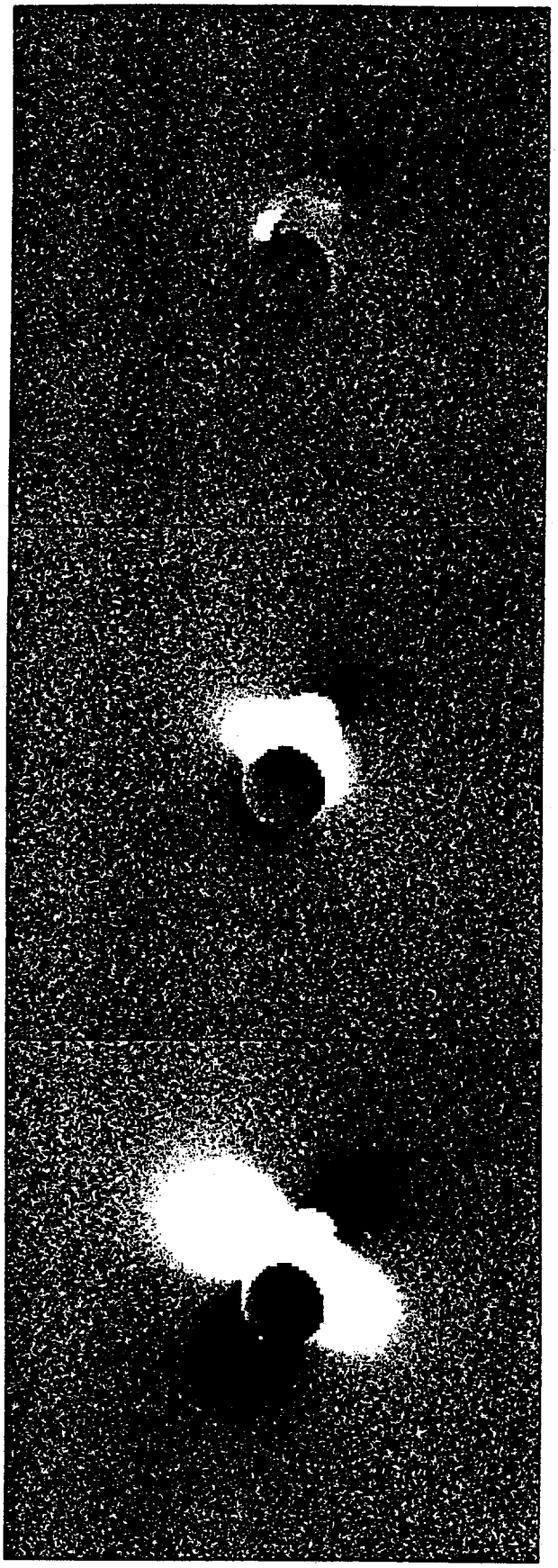

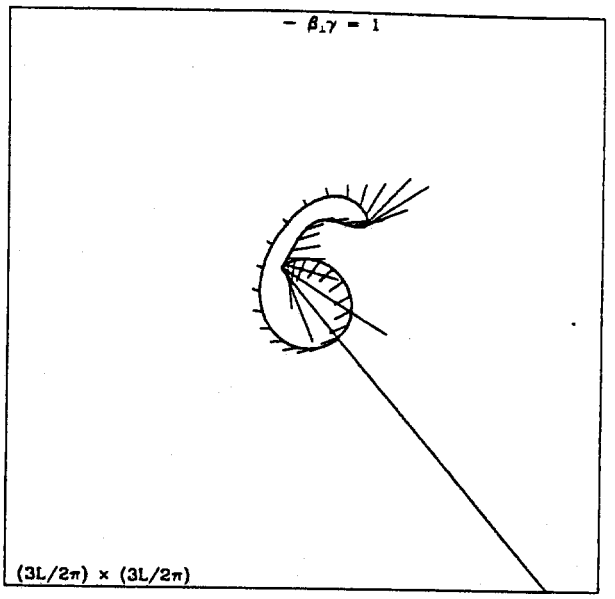

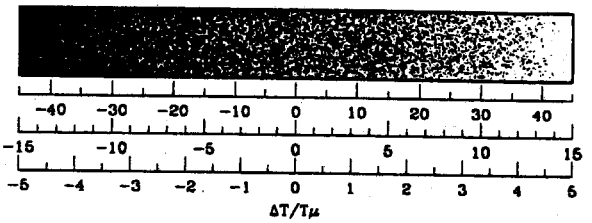

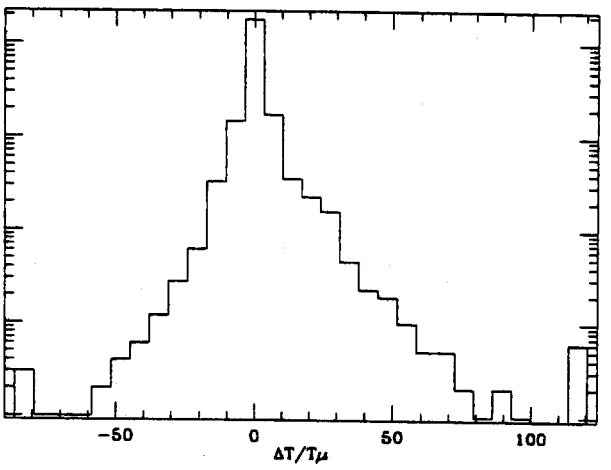

$\langle \Delta T/T \rangle = 0.49\ \mu$

$\langle \Delta T/T \rangle_{rms} = 6.19\ \mu$

$\alpha = 0.50000$

$\sin(\phi) = 0.50000$

$\psi = 100.000$

$\theta_1 = 50.000$

$\theta_2 = 50.000$

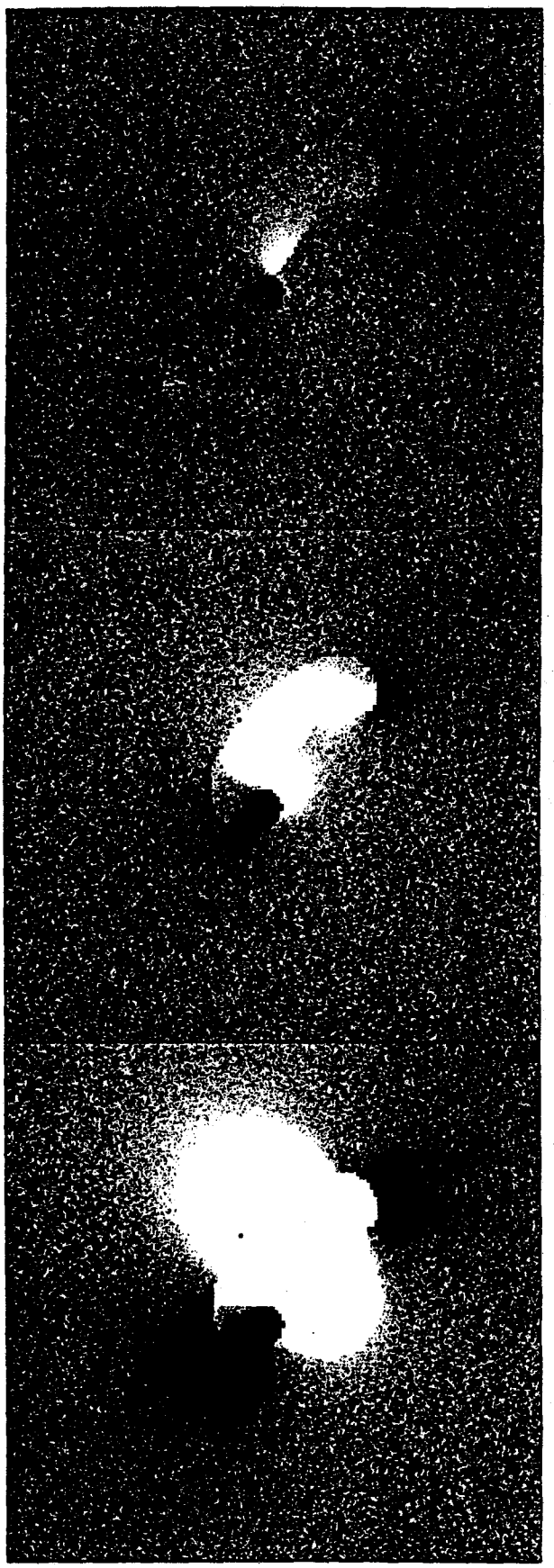

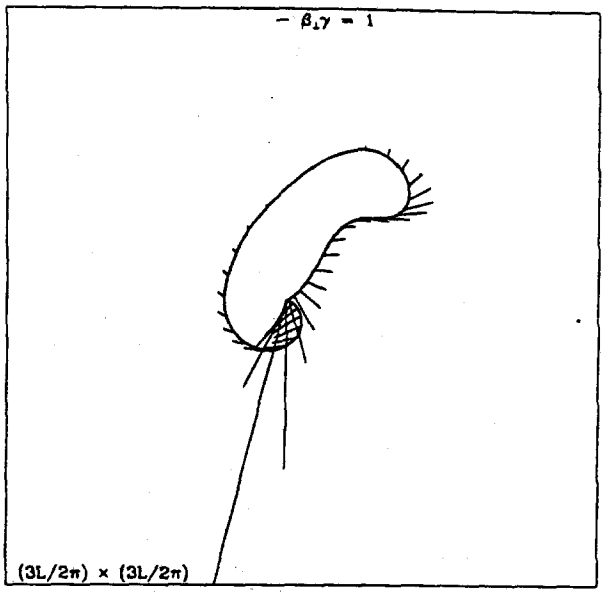

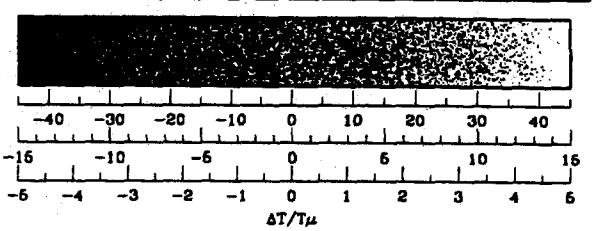

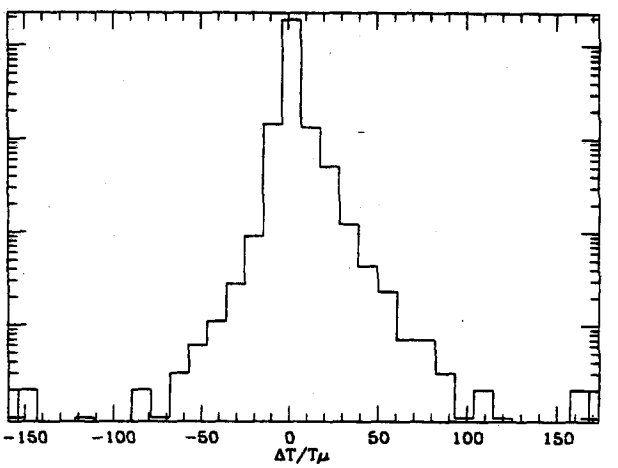

$\langle \Delta T/T \rangle = 1.26\ \mu$

$\langle \Delta T/T \rangle_{rms} = 7.34\ \mu$

$\alpha = 0.50000$

$\sin(\phi) = 0.50000$

$\psi = 120.000$

$\theta_1 = 50.000$

$\theta_2 = 50.000$

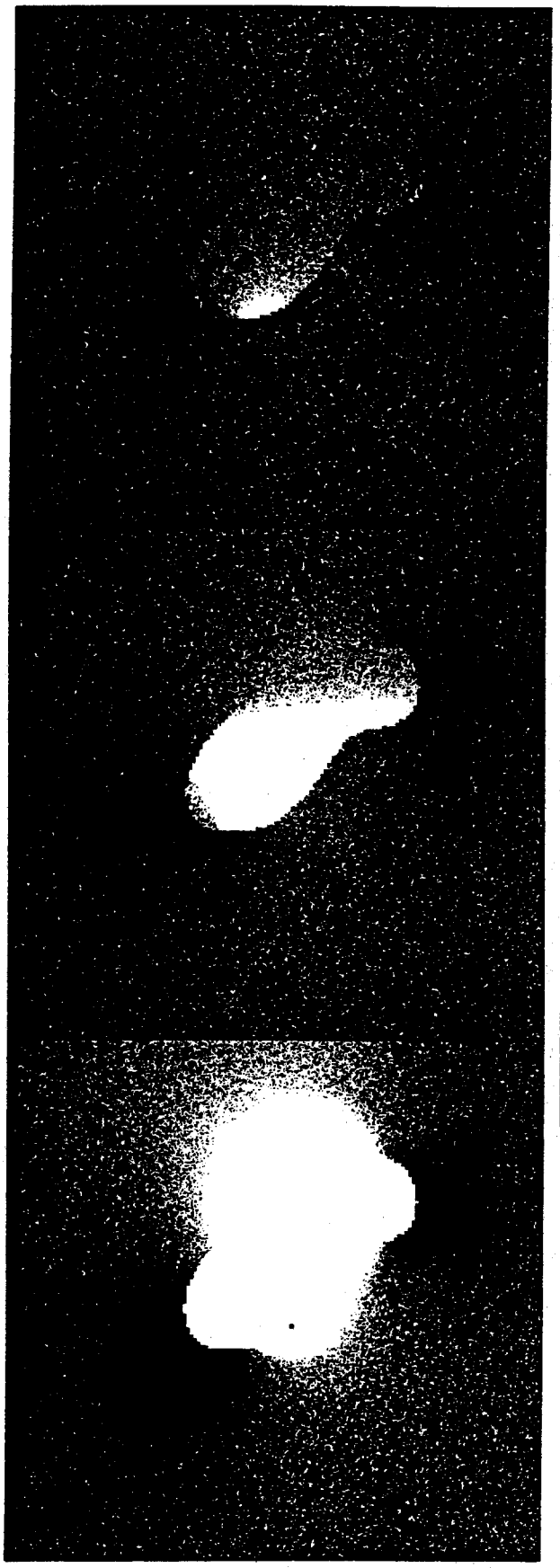

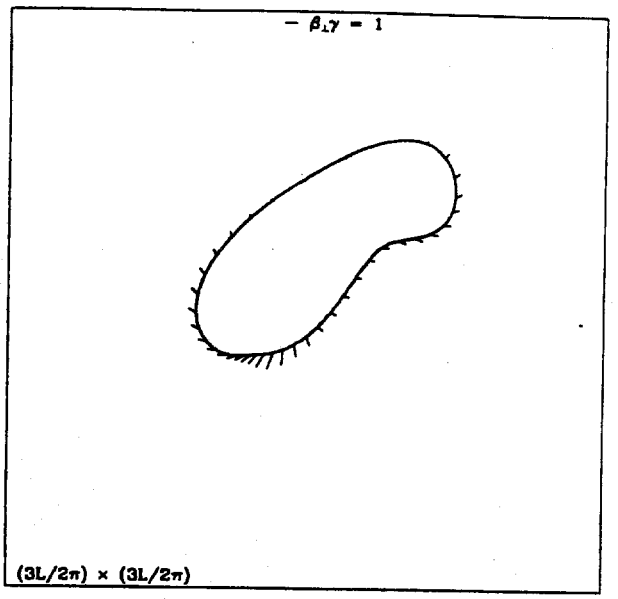

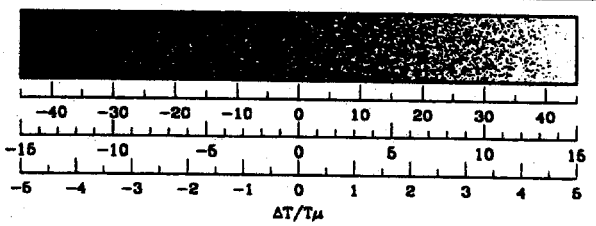

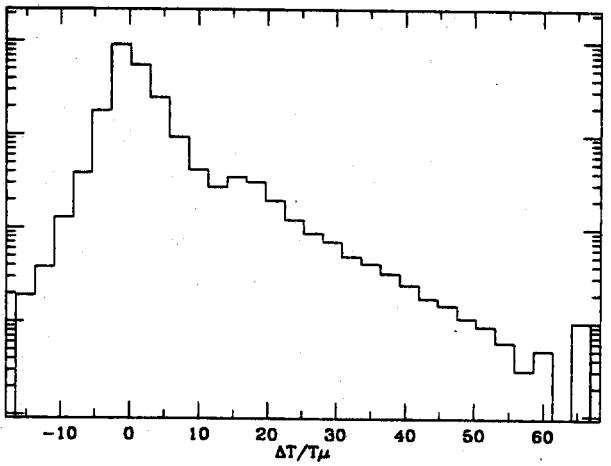

$\langle \Delta T/T \rangle = 1.88\ \mu$

$\langle \Delta T/T \rangle_{rms} = 6.98\ \mu$

$\alpha = 0.50000$

$\sin(\phi) = 0.50000$

$\psi = 140.000$

$\theta_1 = 50.000$

$\theta_2 = 50.000$

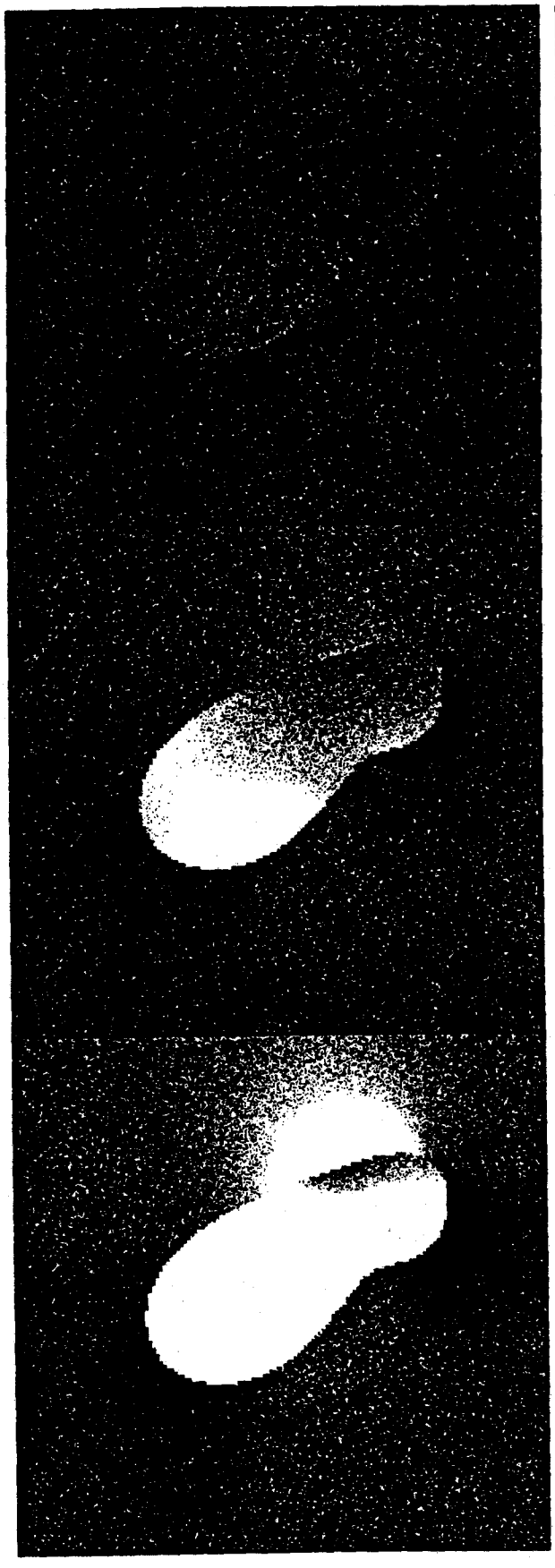

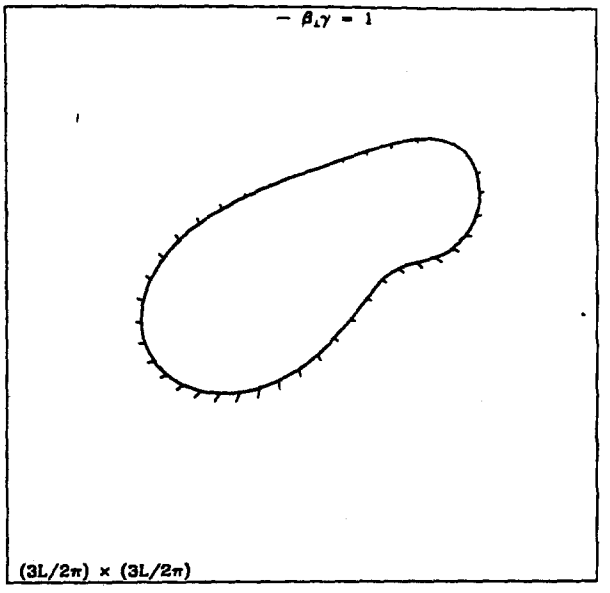

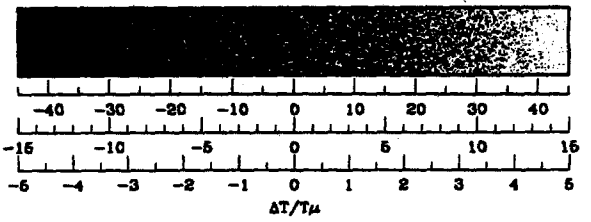

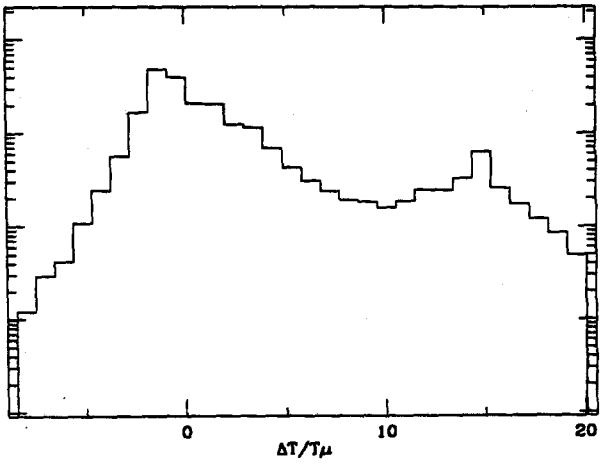

$\langle \Delta T/T \rangle = 1.88\ \mu$

$\langle \Delta T/T \rangle_{rms} = 5.38\ \mu$

$\alpha = 0.50000$

$\sin(\phi) = 0.50000$

$\psi = 160.000$

$\theta_1 = 50.000$

$\theta_2 = 50.000$

failure of their order-of-magnitude estimates are the cancellations discovered in §III of this paper. Given their overestimation of the temperature fluctuations at large impact parameters from a single loop, we must conclude that their subsequent estimates of the statistical properties of anisotropy from an ensemble of loops is incorrect. In particular, their estimates are too high. Calculations of the statistical properties of the microwave anisotropy using the formalism developed in this paper is left to a subsequent paper.

X. SUMMARY

In this paper we have developed a formalism for calculating the microwave background anisotropy from loops much smaller than the horizon. With this formalism calculating the pattern of anisotropy around a given loop at a given time becomes a tractable numerical problem. For each photon trajectory the calculation of the temperature boost is equivalent to a one-dimensional integral over an implicitly defined function. The integral is essentially an integral around the loop. In other words, the integrand may be interpreted as the contribution of a given string particle to the anisotropy of the photon. This result for a string particle is then a simple generalization of the result for a ballistically moving point mass which was calculated using a totally different method by Birkinshaw and Gull (1982). It was also shown that the formalism is identical to a certain class of problems in electrostatics in two dimensions. One may apply this formalism to a face-on circular loop obtaining the result that the anisotropy pattern is a top hat. This is the only case where this author was able to obtain the anisotropy pattern analytically. The discontinuity of temperature across the string, which was first derived by Kaiser and Stebbins (1984) for an infinite straight string, is generalized here to arbitrary string configurations. The pattern of anisotropy around kinks and cusps was also examined. In both cases the temperature deviation becomes large. In the case of kinks it grows only logarithmically with decreasing impact parameter with respect to the cusp. In the case of cusps it grows as the inverse square root of the impact parameter from the cusp. The pattern of anisotropy far from a loop is a dipole pattern which falls off as the inverse of the impact parameter. This is the same result as for a moving point mass. However, the amplitude of the dipole pattern for a loop is not an indication of the total momentum as it is for a point mass. In fact, the amplitude and direction of the dipole pattern will oscillate with the loop. A quadrupole usually dominates just outside the loop. It was shown that the temperature pattern from the effect calculated here obeys the two-dimensional Laplace equation. One consequence of this is that there will be no hot or cold spots except in the direction of a piece of string. Finally, the pattern of anisotropies was calculated for a few specific loop configurations. Typical anisotropies of $5 - 10\,\tilde{\mu}$ near the loop were found. The analysis here suggests that the work of Brandenberger, Albrecht, and Turok (1986) with respect to MBR anisotropy is in error. Their estimates of MBR anisotropy from gravitational waves emitted by loops is too large.

The next step is to try to apply the formalism to put limits on possible string parameters. As mentioned in the text this effort cannot go beyond rough estimates obtained by previous authors without further progress in our understanding of the distribution of strings, especially in the matter era. In a future paper we shall use the results derived here to determine the statistical properties of the anisotropy given the population of loops. Once this is achieved the formalism here may be applied to give a precise interpretation to present and future anisotropy measurements with regard to the existence of cosmic strings. The formal-

ism presented here, however, can only tell us about subhorizon loops in front of the surface of last scattering. The gravitational effects of superhorizon strings must also be calculated, and this may be and is being done, in analogy with the analysis here (Veeraraghavan, Stebbins, and Silk 1987). Of course, the traditional surface of last scattering effects may also be better understood in the string scenario.

ACKNOWLEDGEMENTS

Much of this work was done in partial fulfillment of the requirements for a Ph.D. at the University of California at Berkeley. This work has been supported by NASA and the DOE at Berkeley and at Fermilab.

APPENDIX A. PROOF OF CANCELLATION OF DIVERGENCES

It was shown in §III that in the formula (3.15) the contribution of and individual particle to $\Delta E/E$ is divergent. We now derive an identity, a special case of which is equation (3.20). This is sufficient to prove that the divergences of equation (3.17) cancel. The equation of local energy-momentum conservation is

$$T^{\alpha\beta}{}_{,\beta} = 0.$$

One may integrate the above over the plane $\mathbf{n}\cdot\mathbf{x} = \tau + w$ to obtain

$$\int [T_{\alpha 0,0}(\mathbf{x},t') - T_{\alpha i,i}(\mathbf{x},t')]\delta(\tau - \mathbf{u}\cdot\mathbf{x} + w)\, d^3\mathbf{x} = 0,$$

where $\mathbf{u}$ and w are independent of x and t. Evaluating this at $t' = \tau$ and then integrating over all τ, we find

$$\int [T_{\alpha 0,0}(\mathbf{x},\mathbf{u}\cdot\mathbf{x} - w) - T_{\alpha i,i}(\mathbf{x},\mathbf{u}\cdot\mathbf{x} - w)]\, d^3\mathbf{x} = 0.$$

Finally integrating by parts, we obtain

$$\int [T_{\alpha 0,0}(\mathbf{x},\mathbf{u}\cdot\mathbf{x} - w) + u^i T_{\alpha i,0}(\mathbf{x},\mathbf{u}\cdot\mathbf{x} - w)]\, d^3\mathbf{x} = 0. \tag{A1}$$

If the stress-energy tensor is expressed as, $T_{\alpha\beta}(\mathbf{x},t') = \sum_p T^p_{\alpha\beta}(t')\delta^{(3)}(\mathbf{x} - \mathbf{r}^p(t'))$, as it has been above, then equation (A1) becomes

$$\sum_p \frac{1}{1 - \mathbf{u}\cdot\dot{\mathbf{r}}^p(t^p_*)} \left[\frac{\partial}{\partial t'}\left(\frac{T^p_{\alpha 0}(t') + u^i T^p_{\alpha i}(t')}{1 - \mathbf{u}\cdot\dot{\mathbf{r}}^p(t')}\right)\right]_{t'=t'^p_*} = 0. \tag{A2}$$

Here t'^p_* is implicitly defined by

$$\mathbf{u}\cdot\mathbf{r}^p(t'^p_*) = w \tag{A3}$$

and we shall assume that it exists for each p and is unique. The particle trajectories in which we are interested exist for all times and have velocities less than the speed of light. If this is true, then existence and uniqueness of t'^p_* is guaranteed if $|\mathbf{u}| \leq 1$. A particular case of equation (A2) is when $\mathbf{u} = \hat{\mathbf{k}}$ and $w = \hat{\mathbf{k}}\cdot\mathbf{x}_0$. In this case t^p_* will be equal to $t'^p_{\max}$ defined in equation (3.12) which does exist for all p and is unique. If we then take the scaler product of the resultant equation with the 4-vector $k^\alpha = (1,\hat{\mathbf{k}})$ and divide by 2 we obtain

$$\sum_p \frac{1}{1 - \hat{\mathbf{k}}\cdot\dot{\mathbf{r}}^p(t'^p_{\max})} \left[\frac{\partial}{\partial t'}\left(\frac{S^p(t')}{1 - \hat{\mathbf{k}}\cdot\dot{\mathbf{r}}^p(t')}\right)\right]_{t'=t'^p_{\max}} = 0, \tag{A4}$$

which is equation (3.18). Thus the divergent terms in equation (3.15) sum to zero. However, these divergences would make numerical integrations of equation (3.15) impossible. One must modify equation (3.15) to avoid these divergences altogether.

REFERENCES

A. Albrecht and N. Turok, *Evolution of Cosmic Strings*, *Phys. Rev. Lett.* **54** (1985), 1868.

A. Albrecht, E. Copeland, and N. Turok, in preparation.

M. Birkinshaw and S. Gull, *A Test for Transverse Motions of Clusters of Galaxies*, *Nature* **302** (1983), 315-317.

R. Brandenberger, A. Albrecht, and N. Turok, *Gravitational Radiation from Cosmic Strings and the Microwave Background*, *Nucl. Phys. B* **277** (1986), 605.

R. Brandenberger and N. Turok, *Fluctuations from Cosmic Strings and the Microwave Background*, Phys. Rev. **D33** (1986), 2182.

D. Burstein *et al.*, in "*Galaxy Distances and Deviations from the Hubble Flow*", ed. B. Madore and R. Tully, D. Reidel, Dordrecht, 1986, pp. 123.

S. Chase, *Cosmic Strings, Hydrodynamics, and Microanisotropies in the Cosmic Background Radiation*, Nature **323** (1986), 42.

C. Collins, R. Joseph, and N. Roberston, *Large-Scale Anisotropy in the Hubble Flow*, *Nature* **320** (1986), 506.

R. Davis, *Nucleosynthesis Problems for String Models of Galaxy Formation*, *Phys. Rev.* **D32** (1985), 3172.

P. Goddard, J. Goldstone, C. Rebbi, and C. Thorn, *The Quantum Dynamics of a Massless Relativistic String*, *Nucl. Phys.* **B56** (1973), 109.

R. Gott, *Gravitational Lensing Effects of Vacuum Strings: Exact Solutions*, *Astrophys. J.* **288** (1985), 422.

T. Hara, *Variation of 3K Background Radiation Due to Cosmic Strings*, Prog. of Theor. Phys. **75** (1986), 836.

C. Hogan and M. Rees, *Gravitational Interactions of Cosmic Strings*, *Nature* **311** (1984), 109.

N. Kaiser and A. Stebbins, *Microwave Anisotropy due to Cosmic Strings*, *Nature* **310** (1984), 391.

T. Kibble and N. Turok, *Self-Intersection of Cosmic Strings*, *Phys. Lett* **116B** (1982), 141.

C. Thompson, *On the Dynamics of Cosmic Strings*, Princeton preprint.

J. Traschen, N. Turok, and R. Brandenberger, *Microwave Anisotropy from Cosmic Strings*, *Phys. Rev.* **D34** (1986), 919.

N. Turok, *Grand Strings and Galaxy Formation*, *Nucl. Phys.* **B242** (1984), 520.

N. Turok and R. Brandenberger, *Cosmic Strings and the Formation of Galaxies and Clusters of Galaxies*, *Phys. Rev.* **D33** (1986), 2175.

T. Vachaspati, *Gravitational Effects of Cosmic Strings*, *Nucl. Phys.* **B277** (1987), 593.

S. Veeraraghavan, A. Stebbins, and J. Silk, in preparation.

A. Vilenkin, *Gravitational Field of Vacuum Domain Walls and Strings*, *Phys. Rev.* **D23** (1981), 852.

A. Vilenkin, *Cosmic Strings and Domain Walls*, *Physics Reports* **121** (1985), 263.

S. Weinberg, "*Gravitation and Cosmology*", John Wiley & Sons, New York, 1972.

ALBERT STEBBINS **Fermilab MS 209, Box 500, Batavia, IL 60510**